

Evaluating Optimal Farm Management of Phosphorus Fertilizer Inputs with Partial Observability of Legacy Soil Stocks*

Chanheung Cho Zachary S. Brown David M. Kling Luke Gatiboni Justin S. Baker

May, 2024

Please [click here](#) for the latest draft.

Abstract

This study explores the dynamic management of legacy phosphorus (P) in agricultural systems, focusing on the decision-making processes of farmers applying P fertilizer and soil sampling under legacy soil P state uncertainty. Employing a Mixed Observability Markov Decision Process framework, we examine how the dynamics of partially observable legacy P stocks, coupled with Epstein-Zin preferences for risk aversion and elasticity of intertemporal substitution, influence optimal management decisions. Our findings reveal that higher risk aversion leads to greater P fertilizer application across all levels of legacy P bioavailability. Additionally, as the elasticity of intertemporal substitution increases, indicating a higher preference for intertemporal smoothing, there is a shift toward higher rates of soil sampling to manage uncertainty in legacy P levels more effectively. These findings suggest that farmer risk preferences significantly shape their management strategies, guiding development and policies that could enhance sustainable agricultural practices by optimizing the use of legacy P while mitigating environmental impacts.

JEL Codes: Q15, Q24, C61, C63

Keywords: Legacy Phosphorus, Risk Preference, State Uncertainty, Epstein-Zin Preference, Mixed-Observability Markov Decision Processes

*Cho: North Carolina State University (ccho5@ncsu.edu); Brown: North Carolina State University (zsbrown2@ncsu.edu); Kling: Oregon State University (David.Kling@oregonstate.edu); Gatiboni: North Carolina State University (luke_gatiboni@ncsu.edu); Baker: North Carolina State University (jsbaker4@ncsu.edu). The authors thank participants at various conferences and seminars for useful comments and discussions. Financial Support from the National Science Foundation (NSF) Award #2019435: Science and Technologies for Phosphorus Sustainability.

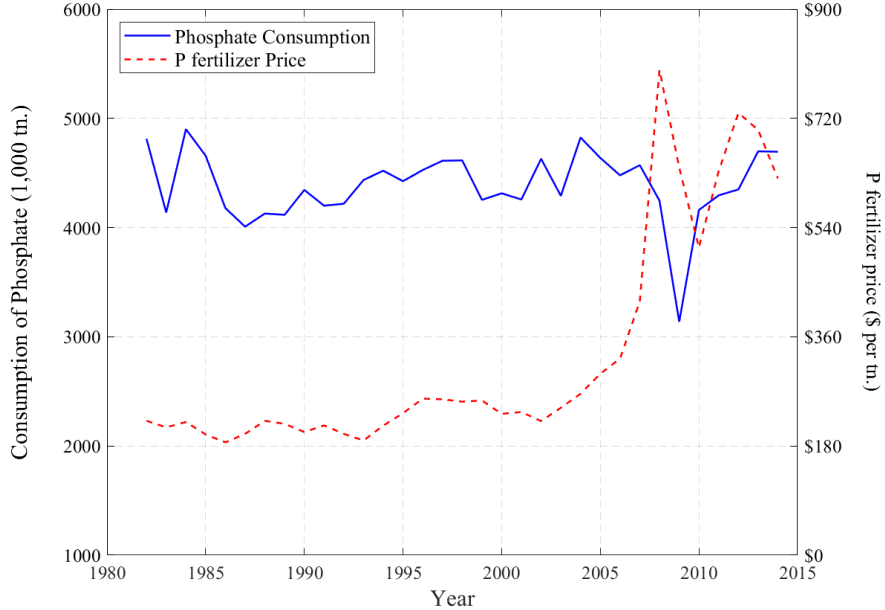
1 Introduction

Economically efficient management of the agricultural nutrient Phosphorus (P) has become a critical global issue for ensuring sustainable crop production and environmental protection. P is imbalanced in the global food system, with some regions lacking sufficient access to synthetic or organic P fertilizers that could boost yields and rural incomes, leaving producers to mine P from nutrient-deficient soils ([Zou et al. 2022](#)). In the United States context (and in other advanced economies) the main social challenge in P management is the excessive application of P fertilizer in farmland, which contributes to water quality degradation problem of P scarcity and overconsumption are intensified by the depletable nature of P and global concerns over dwindling mineral stocks and rising prices. However, as illustrated in Figure 1, P fertilizer consumption by US farmers has remained relatively stable over the last few decades and has evidently responded only temporarily to recent and persistent price increases, suggesting relatively price inelastic demand for P in US cropping systems ([Denbaly and Vroomen 1993](#)).

Notably, unlike nitrogen fertilizer, P fertilizer application residuals after crop take-up can accumulate in soils. This accumulating soil stock of P – referred to as ‘legacy P’ – can be stored in non-bioavailable reserve, be taken up by future crop plantings or be mobilized by subsequent precipitation events, flowing into water bodies. A significant extent of US agricultural land has been estimated to have accumulated legacy P stocks over decades of continuous cultivation application of P from synthetic and organic sources (e.g., annually, > 1,000 tonnes of P have accumulated in the Vermont agricultural region) ([Wironen et al. 2018, Ringeval et al. 2018](#)). P runoff into water bodies catalyzes eutrophication, which create hypoxic ‘dead zones’ and emit Greenhouse Gases (GHG) ([Arrow et al. 2018, Conley et al. 2009, Iho and Laukkonen 2012, Rabotyagov et al. 2014, Paudel and Crago 2020](#)). [Downing et al. \(2021\)](#) estimate a substantial cost associated with GHG emission from eutrophication in freshwater system globally (equivalent to 20% of the emission from global fossil fuel consumption).

Various policies have been proposed to mitigate environmental issues arising from the overuse of P fertilizers, including the Numeric Nutrient Criteria under Clean Water Acts and Binational Phosphorus Reduction Strategy in Lake Erie ([US EPA 1995, Lake Erie LaMP 2011](#)), with one notable proposal focusing on getting farmers to substitute legacy, soil-bound P stocks for P fertilizer and to reduce P fertilizer applications ([Sattari et al. 2012, USDA 2020](#)). Properly managed, bioavailable legacy P stock can support crop growth and prevent the overuse of P fertilizer, reducing costs and environmental impact from fertilizer-intensive crop operations ([Sattari et al. 2012](#)). Yet this policy idea begs the question of why farmers currently

Figure 1: U.S. Phosphorus consumption and phosphorus fertilizer price



Notes: The graph shows the relationship between P fertilizer consumption and P fertilizer prices from 1982 to 2014. The blue solid line represents P consumption, measured in 1,000 short tons on the left y-axis and the red dashed line indicates the price of P fertilizer, measured in dollars per short ton on the right y-axis.

appear for the most part not to utilize legacy P stocks at all (given their accumulation over time), since economists would expect some private incentive to do so to reduce input costs while maintaining yields.

This paper studies this question using a model-based approach to analyze farmers' dynamic incentives to utilize these stocks in a setting of imperfect information. The complexity of managing legacy P stocks poses significant challenges for farmers, and the economic payoffs from different strategies recommended by agricultural extension are uncertain. Recent analysis suggests that farmers may not fully account for these residual P stocks in their decision-making processes, including the quantity of P fertilizer to apply during a given crop growing cycle, due to a lack of information and the inherent uncertainty about the condition and bioavailability of legacy P stocks across their farmland. Particularly when accounting for farmer risk aversion, the uncertainty surrounding legacy P could contribute to its underutilization. This paper explores how these factors shape the dynamic incentives for legacy P utilization and examines whether improved access to enhanced monitoring of legacy P stocks could reduce P fertilizer application.

To address the management of legacy P accumulated in the soil and its losses to surface water, previous studies have analyzed the optimization of fertilizers in farmland along with

P control or conservation policies. [Schnitkey and Miranda \(1993\)](#) analyzed the optimal steady-state application of fertilizer under various policy settings which limit the soil P level. [Goetz and Zilberman \(2000\)](#) examined the intertemporal and spatial optimal application of mineral fertilizer levels given P concentrations in bodies of water associated with agricultural land for optimal lake restoration policy. [Innes \(2000\)](#) explains that environmental impact of nutrient runoff from livestock production can be mitigated by regulating facility size, implementing waste policies based on cleanup costs, and combining fertilizer taxes with subsidies for manure spreading equipment. [Lötjönen et al. \(2020\)](#) provided a theoretical framework and study the P policies associated with climate change through the spatial application of P from mineral and manure fertilizers. While the models in these studies account for optimal fertilizer usage decisions to manage P accumulation in soils and to reduce P loss to the surface water, they do not incorporate the observational uncertainty related legacy P, and thus cannot answer the question we address here.

To address the observational uncertainty, US farmers commonly employ standard soil sampling, provided by state agencies or extension services and by private soil testing service laboratories at nominal fees, to gauge legacy P availability. These tests, when conducted at a limited number of spots within their fields, offer preliminary insight into soil P content, serving as noisy indicators of the actual bioavailable legacy P stock across a field ([Austin et al. 2020](#)). While more comprehensive sampling options exist, offering clearer information, they come at a higher cost, presenting a trade-off between accuracy and expense ([Austin et al. 2020, Gatiboni et al. 2022](#)). Economically, this situation can be described as one in which the agent – here, the farmer – optimizes their utilization of an uncertain resource stock – here, legacy P – in which they may dynamically update their beliefs about these fluctuating stocks based on costly monitoring. Generically, this a common situation in the resource management literature, referred to as a Partially Observable Markov Decision Process or POMDP ([Clark 2010, Fackler and Pacifici 2014, Fackler 2014](#)). Previous applications of POMDP models and extensions in resource management have included invasive species control ([Haight and Polasky 2010, Rout et al. 2014, Kling et al. 2017](#)), forestry ([Sloggy et al. 2020](#)), environmental conservation ([White 2005](#)), erosion prevention ([Tomberlin and Ish 2007](#)), and infectious diseases ([Chadès et al. 2011](#)).

To our knowledge POMDP methods have yet to be applied either in a depletable resource context or in farm production economics (though [Sloggy et al.](#)'s forestry application is adjacent to such a setting), reflecting one contribution of this paper. Previous agricultural economics studies have addressed the partial observability and monitoring problem using more heuristic optimization methods that separate inference about unobserved state variables from the optimization. For example, [Fan et al. \(2020\)](#) employ such an approach using state-space

models to analyze efficient monitoring of an agricultural pest, but they specifically note the theoretical superiority of a POMDP approach for their application were it not for the computational difficulty of these methods.

Additionally, as far as we are aware, agent risk preferences have not previously been included in POMDP or optimal applications, at least in agricultural or resource economics. It is natural to conjecture that risk aversion could strongly affect demand for monitoring and the utilization of uncertain stock dynamics. Our analysis of that general conjecture represents another contribution. Because standard discounted expected utility in dynamic economic models conflates preference parameters for risk aversion and intertemporal substitution, we employ a widely used recursive utility Epstein-Zin specification to disentangle these effects in our analysis ([Epstein and Zin 1991](#)).

We develop our model's empirical foundation using North Carolina field data on legacy P abundance and yield response in a corn-farming context spanning six years, with which we estimate the yield response to both P fertilizer applications and legacy stocks. We also account for stochastic crop and P fertilizer price dynamics, which we jointly estimate using publicly available USDA data. We also include stochastic crop and fertilizer prices which extend the model into what are known as Mixed Observability Markov Decision Processes (MOMDPs) ([Kovacs et al. 2012](#), [Sloggy et al. 2020](#)). Inclusion of these dynamics increases the robustness of our analysis, given that previous studies show that stochastic price dynamics have important effects on other dynamic farm resource management problems, such as crop rotation and cover crop planting ([Livingston et al. 2015](#), [Chen 2022](#)).

Including all the elements described above is a significant computational challenge. In particular, POMDPs involve stochastic dynamic programming in which the agents possess belief states that specify their current subjective probability distributions about imperfectly observed biophysical states, with these beliefs states updated via Bayes' Rule. The specification introduces a high-dimensional state space (i.e. a space of probability distributions) that imposes considerable barriers on numerical computation. To address this problem, we closely follow recently applied density projection methods (e.g. [Zhou et al. 2010](#), [Springborn and Sanchirico 2013](#), [MacLachlan et al. 2017](#), [Kling et al. 2017](#), [Sloggy et al. 2020](#)) that reduce the dimensionality of the belief states, while avoiding some of the restrictions and pitfalls of prior methods (e.g. use of conjugate priors or coarse discretization of the unobserved state).

Our study reveals that higher risk aversion among optimizing farmers generally decreases the reliance on legacy P stocks in favor of fertilizer application. Demand for enhanced monitoring is also affected by the farmer's degree of risk aversion, but in nonmonotonic ways that also interact with preferences for intertemporal smoothing. Utilization of legacy P and demand for monitoring also tends to increase with farmer tolerance for intertemporal

substitution, especially when risk aversion is low. Furthermore, sensitivity analysis with much higher fertilizer prices (e.g. from a fertilizer tax or sustained global market disruption) or much lower monitoring costs (e.g. from a subsidy) do not induce much additional use of legacy soil P. Taken together, these results highlight the challenge of developing effective policy incentives to promote additional legacy P.

This paper's sections proceed as follows. First, the dynamics of legacy P are described, detailing the model's structure and equations, which capture both the accumulation and bioavailability of legacy P. Next, the economic and management problems are discussed, outlining how farmers can evaluate the recursive expected utility of their controls, P fertilizer application, and soil sampling in the face of stochastic prices and the unobservable state of legacy P. Then, the methodological framework and specification are presented, including price dynamics and the density projection approach for managing Bayesian belief updating. The application of this model to the corn market provides a practical example of how it can be used to guide decision-making in agriculture. Finally, the results of the model are discussed and are integrated with Epstein-Zin preferences, highlighting the implications of risk preferences in shaping farmers' P fertilizer application and soil sampling decisions.

By addressing both the economic decisions associated with agricultural production and the biophysical aspects of legacy P management, this paper provides valuable insights for policymakers and researchers interested in P sustainability in agricultural systems.

2 Model Description

A model of optimal management for legacy P is presented that incorporates uncertainties of both the legacy P status and stochastic pricing. Farmers' primary objective is to maximize the crop yields through actions that involve two control variables: P fertilizer application and soil sampling. During each decision period, farmers observe current legacy P levels and crop prices and then choose P fertilizer application levels and decide whether to employ soil sampling. The information derived from the controls is used for updating beliefs about the status of legacy P.

2.1 Legacy Phosphorus Dynamics Model

The model in this paper closely follows that of [Iho and Laukkanen 2012](#), with the addition of stochastic carry-over properties. The model describes the average accumulated legacy P

per hectare given by L_t with the change in legacy P status shown in equation (1):

$$L_{t+1} = \rho_t L_t + (\gamma_1 + \gamma_2 L_t) \underbrace{\left[F_t - \frac{\text{Concentration on Yield}}{(\gamma_3 \log(L_t) + \gamma_4)} Y(L_t, F_t) \right]}_{\text{Legacy P Surplus}} \quad (1)$$

where ρ_t denotes the carry-over parameter of legacy P, F_t represents the amount of P fertilizer input, and $Y(L_t, F_t)$ is the crop yields at time t . The terms $(\gamma_3 \log(L_t) + \gamma_4)$ defines the legacy P concentration of the crop yield, which increases logarithmically with L_t . As L_t increases, the legacy P concentration also rise, initially leading to augmented yields. However, despite ongoing increases in L_t , the marginal yield gains attribute to each additional unit of legacy P progressively diminish. The term $(\gamma_1 + \gamma_2 L_t)$ is the legacy P balance scaling factor that scales the effect of the legacy P balance on the change in L_{t+1} ([Ekholm et al. 2005](#)). The parameter values of γ are summarized in Table 2.

While there are several ways to introduce uncertainty into dynamics resource allocation models, our dynamics model concentrates on introducing uncertainty into the carry-over of legacy P. In a deterministic environment, the carry-over parameter is less than one, which characterizes the gradual reduction of the P reserve over time ([Ekholm et al. 2005](#), [Iho and Laukkonen 2012](#)). Here, we assume that the carry-over parameter is a diminishing stochastic multiplier with resource abundance:

$$\rho_t = \exp \left[\left(\mu_\rho - \frac{\sigma_\rho^2(L_t)}{2} + \sigma_\rho(L_t) W_t \right) \right], \quad \text{with } W_t \sim \mathcal{N}(0, 1), \quad (2)$$

where μ_ρ is the log mean percentage rate of growth/decay in L_t and $\sigma_\rho(L_t)$ is the standard deviation of this log percentage growth rate. We assume $\mu_\rho < 0$ meaning the legacy P stock L_t stochastically decay without added P fertilizer or uptake by crop. We specify the degree of stochasticity in growth rate as $\sigma_\rho^2(L_t) = \ln(1 + \varsigma^2/L_t^2 M_\rho^2)$ where ς is an uncertainty coefficient and $M_\rho = \mathbb{E}[\rho_t | L_t]$, which keeps the stochastic behavior of the legacy P stock more realistic, by preventing the conditional variance in next-period stock from growing without bound as L accumulates ([Loury 1978](#), [Gilbert 1979](#), [Melbourne and Hastings 2008](#), [Sims et al. 2017](#), [Sloggy et al. 2020](#)).¹ We also consider a fixed variance scenario ($\sigma_\rho(L_t) = \varsigma$) in the Appendix.

¹Given that $W_t \sim \mathcal{N}(0, 1)$, using the moment generating function of the normal distribution, the $\mathbb{E}[\rho_t | L_t]$ is given by $\mathbb{E}[\rho_t | L_t] = \exp[(\mu_\rho - \sigma_\rho(L_t)^2/2) + \sigma_\rho(L_t)^2/2] = \exp(\mu_\rho)$. This result shows that M_ρ simplifies to a constant that does not depend on L_t when considering the expectation with respect to the normal distribution of W_t .

2.2 Economics and Management Problem

Annual payoffs in the model are evaluated as the profit determined by crop yields and stochastic prices. Formally the expected (partial) profit is specified as the per hectare production function $Y(L_t, F_t)$ and stochastic prices:

$$\pi(L_t, F_t, P_{t+1}^Y, P_t^F, s_t) = P_{t+1}^Y Y_t(L_t, F_t) - P_t^F F_t - c_s s_t, \quad (3)$$

where P_{t+1}^Y and P_t^F are prices for the crop and P fertilizer, respectively, and c_s is a soil sampling cost. The variable s_t reflects the adoption of soil sampling at time t , where a value of one indicates soil sampling adoption and zero indicates no adoption. Fertilizer application decisions are based on the known fertilizer price P_t^F at the time of application, whereas the crop price P_{t+1}^Y will only be realized at the end of the season, is not yet observed at the time of applying fertilizer. This means that the decision to apply fertilizer is informed by the current fertilizer price and the last harvest's crop price, with the upcoming season's crop price P_{t+1}^Y yet to be realized by the end of the season.

In research on resource management utilizing stochastic prices, it is common to model the price dynamics as an autoregressive process to describe certain time series models, due to their simplicity and efficiency in handling linear relationships. However, a range of economic and environmental factors significantly influence crop and fertilizer prices, making traditional autoregression processes insufficient due to their constant parameterization and limitation in capturing the non-linear dynamics characteristic of the market. For instance, favorable weather conditions, which lead to crop abundance, typically result in lower volatility, thereby keeping prices relatively constant. Conversely, adverse weather, global trade, or geopolitical conditions may lead to supply scarcity and result in higher volatility, increasing price fluctuations. These varying conditions and their impact on crop and P fertilizer prices demonstrate the non-linear and regime-dependent nature of the process.

Markov-Switching Dynamic Regression (MSDR) models, with their ability to incorporate multiple regimes within their processes, provide a more robust framework using regime-dependent parameters. A MSDR model allows for the probability of switching between different regimes according to the Markov process ([Hamilton 1989](#)), each with its own distinct economic and environmental characteristics. When the process is in regime r_{t+1} at time $t + 1$, we model the crop and P fertilizer prices as:

$$\begin{aligned} \ln(P_{t+1}^Y) &= \alpha_{0,r_{t+1}} + \alpha_{1,r_{t+1}} \ln(P_t^Y) + \alpha_{2,r_{t+1}} \ln(P_t^F) + \epsilon_{t+1} \\ \ln(P_{t+1}^F) &= \beta_{0,r_{t+1}} + \beta_{1,r_{t+1}} \ln(P_t^F) + \beta_{2,r_{t+1}} \ln(P_t^Y) + v_{t+1} \end{aligned} \quad (4)$$

where $\alpha_{0,r_{t+1}}, \beta_{0,r_{t+1}}$ are the intercepts for price regime r_{t+1} and ϵ_{t+1}, v_{t+1} are the identical distribution (i.i.d.) normal errors with mean zero and regime-dependent variance $\sigma_{\epsilon,r_{t+1}}^2, \sigma_{v,r_{t+1}}^2$, respectively. In the MSDR, the probability of regime r_{t+1} can be specified as $p_{ij} = \Pr(r_{t+1} = i|r_t = j)$ where p_{ij} represents the probability of transition from regime j at time t to regime i at time $t + 1$ (Hamilton 1989). To maintain tractability, we assume that farmers perfectly observe the price regime they are in, despite the theoretical complexity of this assumption adding another layer of partial observability to the model's dynamics.

Incorporating the dynamic interdependencies between crop price and P fertilizer price into the MSDR model, more accurately reflects intertemporal relationships in price processes. Crop price changes, influenced by the price of P fertilizer, necessitate the inclusion of P_t^F as input cost. Similarly, recognizing the financial planning cycle in agriculture, in which the decision to purchase P fertilizer is based on profits from one years prior, we incorporate P_t^Y to show the economic cycle of P fertilizer purchase decisions.

Legacy P is not perfectly observed, but farmers can receive the information both by soil sampling and adjusting P fertilizer application and observing crop response. Famers obtain the observation O_t about legacy P stocks as they make their fertilizer application decisions. The observation O_t is determined as follows:

$$O_t^l = \begin{cases} L_t + \lambda_t^l & \text{if } L_t > -\lambda_t^l \\ 0 & \text{if } L_t \leq -\lambda_t^l \end{cases} \quad \text{where } \lambda_t^l \sim \mathcal{N}(0, \sigma_l^2). \quad (5)$$

This specification truncates the observation at the zero from below. It also keeps the variance of the observation error conditional on L_t from growing with the level L_t . Together, these assumptions are meant to stylistically reflect the nature of soil sampling, including minimum detectable level and at sufficiently high levels of L an absolute margin of error that is effectively fixed. Here the $l = \{s, F, n\}$ denotes the controls, representing soil sampling (s), P fertilizer application (F), and no controls (n). λ_t^l is an i.i.d. sequence of observation error given by the controls:

$$\lambda_t^l = \begin{cases} \lambda_t^s & \text{if } s_{t-1} = 1 \\ \lambda_t^F & \text{if } F_{t-1} > 0 \text{ and } s_{t-1} = 0 \\ \lambda_t^n & \text{if otherwise.} \end{cases} \quad (6)$$

Our observation equation employs the methodology of Zhou et al. (2010) with the addition of the non-negative observation properties and we assume that the error variance is greater when famers apply P fertilizer, as indicated by $\sigma_F > \sigma_n > \sigma_s$. This assumption is based

on the understanding that the variability of legacy P accumulation is associated with P fertilizer usage. The application of P fertilizer reflects complex biogeochemical interaction in the soil, including weather conditions, nutrient profile, and crops response to these changes, contributing to the increased observation error compared to no controls.

The farmer's beliefs about the distribution of legacy P are denoted as $b_t(L_t)$, representing a subjective probability distribution over the unobserved L_t , conditional upon the history of controls and resulting observations (Kling et al. 2017). Bayesian updating of these beliefs, combining each period's prior belief with new information, is given by:

$$b_{t+1}(L_{t+1}) \propto p(O_{t+1}^l | L_{t+1}, F_t, s_t) \int p(L_{t+1} | L_t, F_t, s_t) b_t(L_t) dL_t \quad (7)$$

with a given $b_0(L_0)$ specifying the prior beliefs about initial stocks and where $p(O_{t+1}^l | L_{t+1}, F_t, s_t)$ is the conditional probability distribution of the observation, as determined from equations (5) and (6). The Markovian properties ensure that the next period beliefs only depend on the current beliefs, controls, and information gained in the current period. The Bellman equation for the recursive expected utility function is follows:

$$V(\mathbf{S}_t) = \max_{F,s} C(\mathbf{S}_t, F_t, s_t) + \beta \mathbb{E}\{V(\mathbf{S}_{t+1}) | \mathbf{S}_t, F_t, s_t\}, \quad (8)$$

where β is the discount factor and $\mathbf{S}_t \equiv [b_t(L_t), P_t^Y, P_t^F]$ is the vector, which includes the current belief distribution of legacy P stock and the prices of crop and fertilizer at time t. Specially, P_t^Y represents the last observed crop price at the beginning of the growing season, i.e. last season's crop price at harvest. $C(\mathbf{S}_t, F_t, s_t)$ is the certainty-equivalent payoff for over uncertain end-of-season profits $\pi(L_t, F_t, P_{t+1}^Y, P_t^F, s_t)$:

$$C(\mathbf{S}_t, F_t, s_t) \equiv \iint \pi(L_t, F_t, P_{t+1}^Y, P_t^F, s_t) b_t(L_t) f(P_{t+1}^Y | P_t^Y, P_t^F) dL_t dP_{t+1}^Y \quad (9)$$

where $f(P_{t+1}^Y | P_t^Y, P_t^F)$ is conditional probability density function of crop price P_{t+1}^Y at the upcoming harvest, given the last observed harvest price P_t^Y and the current fertilizer price P_t^F . In addition, we develop the MOMDP model for managing legacy P by integrating Epstein-Zin preferences into the dynamic programming mapping process, allowing for a more precise depiction of risk premiums distinct from an individual's intertemporal substitution preferences (Lybbert and McPeak 2012). The Bellman equation for the recursive expected utility function, given Epstein-Zin preferences, is as follows:

$$V_{EZ}(\mathbf{S}_t) = \max_{F,s} \left[(1-\beta) C_{EZ}(\mathbf{S}_t, F_t, s_t)^{1-\psi^{-1}} + \beta \mathbb{E}\{V_{EZ}(\mathbf{S}_{t+1})^{1-\eta} | \mathbf{S}_t, F_t, s_t\}^{\frac{1}{1-\eta}} \right]^{\frac{1}{1-\psi^{-1}}}, \quad (10)$$

where $C_{EZ}(\mathbf{S}_t, F_t, s_t)$ is the certainty-equivalent payoff of Epstein-Zin preferences:

$$C_{EZ}(\mathbf{S}_t, F_t, s_t) \equiv \left(\iint \pi(L_t, F_t, P_{t+1}^Y, P_t^F, s_t)^{1-\eta} b_t(L_t) f(P_{t+1}^Y | P_t^Y, P_t^F) dL_t dP_{t+1}^Y \right)^{\frac{1}{1-\eta}} \quad (11)$$

and where η and ψ indicate, respectively, relative Risk Aversion (RA) and Elasticity of Intertemporal Substitution (EIS).

Note that one of the state variables in this model is the entire belief function $b_t(\cdot)$, which makes the dynamic programming problem intractable in its current form. Various methods have been proposed to reduce the dimensionality of beliefs in POMDP, the simplest of which is to use conjugate prior $b_t(\cdot)$ and likelihood function $p(\cdot)$, so that $b_{t+1}(\cdot)$ belongs to the same family as $b_t(\cdot)$ (e.g. normal distribution), reducing the beliefs to simply the parameters of that family (e.g. mean and variance of normal distribution). However, the conjugacy assumption is overly restrictive for most modern resource management problems. The prevailing alternative in the resource economics literature is the density projection method described below.

2.3 Density Projection Approach and Particle Filtering

Continuous state POMDP has challenges due to an infinite-dimensional belief space and because approximating belief states by discretization can lead to computational issues. Exact evaluation of the posterior distribution is difficult to address, and even structuring the belief updating process in discretized space is often infeasible. To address this challenge, a density projection technique suggested by Zhou et al. (2010) and employed by Kling et al. (2017) in economics is utilized.

Density projection projects the infinite-dimensional belief space onto a low-dimensional parameterized family of densities.² Projection mapping from the belief state $b(L)$ to exponential family of density $f(L; \theta)$, where θ is a natural parameter, is achieved by minimizing the *Kullback-Leibler* (KL) divergence between $b(L)$ and $f(L; \theta)$ as:

$$\begin{aligned} b^P(L) &\triangleq \arg \min_f D_{KL}(b \| f) \\ \text{where } D_{KL}(b \| f) &\triangleq \int b(L) \log \frac{b(L)}{f(L; \theta)} dL \end{aligned} \quad (12)$$

$$\forall L, b(L) > 0 \leftrightarrow f(L; \theta) > 0$$

²Technical interpretation of density projection and particle filtering hereafter closely follows Zhou et al. (2010).

and thus belief $b(L)$ and its projection $f(L; \theta)$ satisfies:

$$\mathbb{E}_b[T_j(L)] = \mathbb{E}_\theta[T_j(L)] \quad \text{for } j = 1, 2, \dots, J \quad (13)$$

where $T(L)$ is the sufficient statistics of the probability density (Zhou et al. 2010).

Bayesian updating of projected belief state is implemented adopting a particle filtering, which uses a Monte Carlo simulation approach to estimate the belief state with a limited set of particles (samples) and simulates the transition of the belief state (De Freitas 2001, Arulampalam et al. 2002). In the particle filtering, particles L_t^i for $i = 1, 2, \dots, Z$ are drawn from $b_t(L_t)$ and L_{t+1}^i from the propagation $p(L_{t+1}|L_t, F_t, s_t)$. This allows for the approximation of $b_{t+1}(L_{t+1})$ by the probability mass function (Zhou et al. 2010):

$$b_{t+1}(L_{t+1}) \approx \sum_{i=1}^Z \tau_{t+1}^i \phi(L_{t+1} - L_{t+1}^i) \quad (14)$$

where $\tau_{t+1}^i \propto p(O_{t+1}^l | L_{t+1}^i, F_t, s_t)$, denoting the associated weight and ϕ represent the Kronecker delta function. Substituting equation (13) into (14), the approximation becomes:

$$\begin{aligned} \mathbb{E}_{b_{t+1}}[T_j(L_{t+1})] &= \int T_j(L_{t+1}) b_{t+1}(L_{t+1}) dL_{t+1} \\ &\approx \int T_j(L_{t+1}) \left[\sum_{i=1}^Z \tau_{t+1}^i \phi(L_{t+1} - L_{t+1}^i) \right] dL_{t+1} \\ &= \sum_{i=1}^Z \tau_{t+1}^i T_j(L_{t+1}^i) \\ &= \mathbb{E}_{\theta_{t+1}}[T_j(L_{t+1})] \end{aligned} \quad (15)$$

simplified by the properties of the Kronecker delta function. Thus, if the particles L_t^i are drawn from the projected belief state $b_t^P = f(\cdot; \theta_t)$ and their propagation L_{t+1}^i satisfy the $\sum_{i=1}^Z \tau_{t+1}^i T_j(L_{t+1}^i) = \mathbb{E}_{\theta_{t+1}}[T_j(L_{t+1})]$, the transition probability of θ_t to θ_{t+1} can be calculated.

Density projection effectively reduces infinite-dimensional density to low-dimensional, parameter-defined density, transforming the belief MDP into a more manageable and solvable form referred to as ‘projected belief MDP’. In this paper, the legacy P states are defined as the natural parameters of log-normal distribution and transform to the θ in the ‘projected belief MDP’ calculation (Kling et al. 2017). The parameter transformation and particle filtering algorithms are noted in the Appendix. The utilization of the log-normal distribution in parameterized density is particularly advantageous, primarily due to its tractability to positive-valued state variables and its parametric simplicity characterized by two parameters:

mean and coefficient variation ([Sloggy et al. 2020](#)).

While there are numerous ways to solve the projected belief MDP, we follow [Kling et al. \(2017\)](#) and discretize the projected belief MDP space into a discrete-state space. Because the value function in equations (8) and (10) is a function both of the belief and price states, we then compute the value function on a grid of all discretized possible belief and price state combinations. The details of dynamic programming and numerical algorithm are described in the Appendix.

3 Application to a Representative NC Corn Research Trial

The previous sections presented the model for optimal management of legacy P under unobservable bioavailability to influence crop yield. For the numerical simulation, we apply this model to representative eastern North Carolina corn farm using field trial data ([Morales et al. 2023](#)). To specify crop yield response to fertilizer and legacy P input, we adopt a functional form introduced by [Myyrä et al. \(2007\)](#), and then estimate the parameters of this function using the field trial data:

$$Y_t(L_t, F_t) = \underbrace{\kappa_1 [1 - \kappa_2 \exp(-\kappa_3 L_t)]}_{\text{Response to Legacy P}} + \underbrace{\chi_1 + (\chi_2 - \chi_3 L_t) \sqrt{F_t} + \frac{(\chi_4 - \chi_5 F_t) F_t}{L_t}}_{\text{Response to P Application (mediated by Legacy P)}} + \epsilon_t^Y. \quad (16)$$

The yield response function is comprised of two parts, including the parameters κ and χ , each part reflecting a different aspect of corn yield response. The first part represents the influence of legacy P status on yield, which can explain the independent impact of current legacy P levels. The second part describes the response to the current P application. Specifically, this part is also a function of legacy P, illustrating diminishing marginal productivity with respect to legacy P status ($\partial Y_t / \partial F_t > 0$, $\partial^2 Y_t / \partial F_t^2 < 0$, and $\partial^2 Y_t / \partial F_t \partial L_t < 0$).³ Thus, as legacy P levels increase, the marginal effects of additional P applications on yield tend to decrease. This aspect reflects the non-linear aspect of nutrient application dependent on existing soil conditions.

To estimate the parameters in the yield response function, the data from 5 years of field experiments (2010, 2012, 2014, 2021, and 2022) that examined soil sampling, legacy P bioavailability measured by Mehlich 3 method and reported in milligrams per cubic centimeter of soil (mg/dm^3), P fertilizer application (kg/ha), and yield response of corn production (kg/ha) in the North Carolina Tidewater Research Station were used.

³Figure B1 shows the diminishing marginal return and interaction effect of corn yield function $Y_t(L_t, F_t)$ based on estimated parameters in this section.

Table 1: Nonlinear least square estimation for corn yield

Corn Yield (kg/ha)	
Corn yield response parameter to legacy P	
κ_2	0.657*** (0.245)
κ_3	0.002 (0.011)
Corn yield response parameter to P application	
χ_2	-576.366* (345.467)
χ_3	-2.692 (1.771)
χ_4	10409.78*** (2383.184)
χ_5	42.979*** (7.113)
Obs.	139
Adj. R-squared	0.3980
Root MSE	2292.573

Notes: Clustered standard errors in parentheses. The standard errors are adjusted for clustering in soil sampling ID. $\chi_1 = 0$ is used as a constant term during the estimation. *, **, and *** denote significance at the 10%, 5%, and 1% levels, respectively.

For the soil sampling, two soil sampling methods are considered: standard soil sampling and point soil sampling. Standard sampling collects one soil sample per acre, while point sampling collects multiple samples at specific grid points or random locations within grid cells, typically with four composition samples per acre ($1/4$ -acre grid) (Austin et al. 2020). Thus, point sampling provides more precise information on legacy P bioavailability but is a more expensive methodology to implement. Based on this information, we assumed that the observation error variance of point sampling (σ_p) was smaller than standard sampling ($\sigma_s > \sigma_p$), and the cost was four times higher than standard sampling ($c_p = 4c_s$). The values for the observation errors are denoted in Table 2.

To estimate the parameters in equation (16), a non-linear least square (NLS) was performed using the field trial data. The estimated parameters are summarized in Table 1 and biological

Table 2: Parameters and description

	Value	Description
Biological Parameters		
μ_ρ	-0.02	Average rate of growth (Myyrä et al. 2007)
ς	3	Uncertainty coefficient
γ_1	0.0032	Legacy P balance parameters (Ekholm et al. 2005)
γ_2	0.00084	
γ_3	0.000186	Legacy P surplus parameters (Iho and Laukkanen 2012)
γ_4	0.003	
Economic Parameters		
κ_1	6024.5	75th percentile (Iho and Laukkanen 2012) of observed corn yields for North Carolina sample
c_s	\$67.968	Standard soil sampling cost per ha. (\$27.5 per acre)
c_p	$c_p = 4c_s$	Point soil sampling cost per hectare
β	0.9345	Discount factor with 8% discount rate (Duquette et al. 2012)
σ_F	1.5	Observation error of P fertilizer application without soil sampling
σ_n	1	Observation error of none of controls
σ_s	0.2	Observation error of standard soil sampling
σ_p	0.05	Observation error of point soil sampling

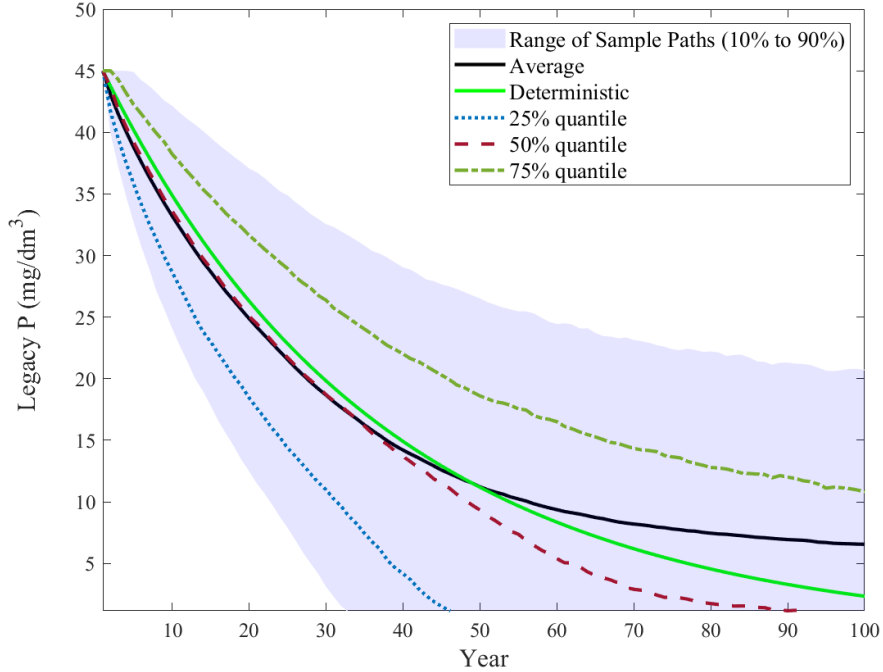
Notes: Soil sampling cost varies depending on the institute. This paper uses the median value of North Carolina case ([Austin et al. 2020](#), \$10 per acre) and California Case ([UC Davis Analytical Lab](#), \$45 per acre).

and other economic parameters are presented in Table 2.

Figure 2 displays the simulation results of legacy P accumulation (mg/dm³) over 100 years without P fertilizer application, illustrating the range of stochastic paths.⁴ The solid green line represents the deterministic path with 2% decay rate that assumes no uncertainty in legacy P dynamics. The shaded area represents the range of simulation sample paths from the 10% to 90% quantile, which becomes broader as the legacy P extends further into the future. Quantile lines for the 25% (blue dots), 50% (red dash-dots), and 75% (green dashes) show the distribution of accumulation, with the 50% quantile also indicated as the median path. The black line represents the average of all simulation results.

⁴The results depicted in Figure 2 were generated from 10,000 simulations.

Figure 2: Legacy phosphorus accumulation without phosphorus fertilizer application



Notes: For the deterministic legacy P accumulation (green solid line), we employ a constant carry-over parameter $\rho_t = \rho = 0.98$ (2% decay rate) as adopted by [Myyrä et al. \(2007\)](#).

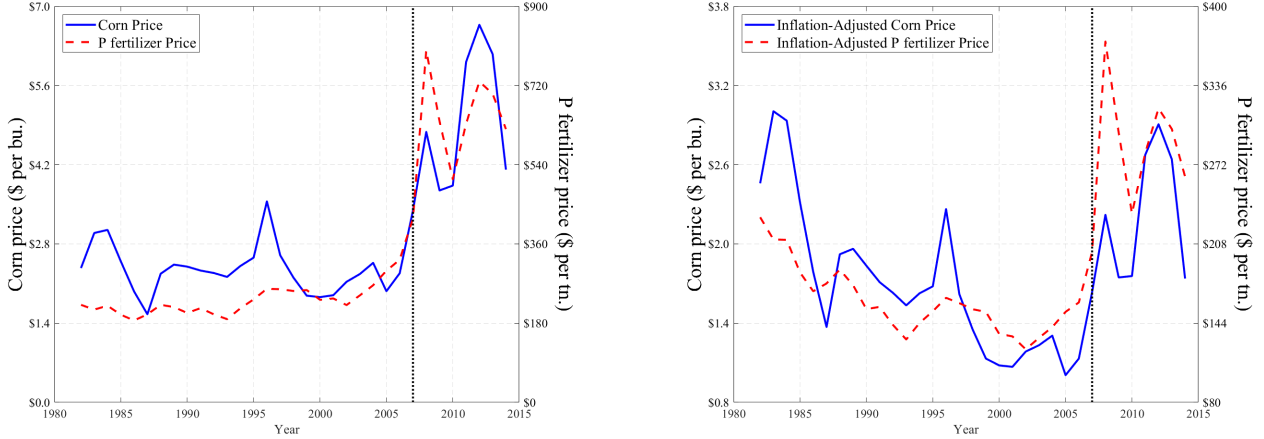
4 Results

In this section, the solution corresponding to the management model introduced in the previous sections, including state uncertainty and price stochasticity, is presented. First, we present results from empirical analysis of prices and from estimation of yield response.

4.1 Price Dynamics and Regime Switching

To analyze price stochasticity, we used P fertilizer (44%-46% phosphate) price data from the USDA “Fertilizer Use and Price” report and sourced corn price data from the USDA’s “U.S. Bioenergy Table” ([USDA 2024a](#), [USDA 2024b](#)). The P fertilizer and corn price data spanned 33-years (1982-2014). Figure 3 shows the nominal and real prices over the observed periods. The solid blue lines represent the corn price per bushel (per bu.), and the dashed red lines indicate the P fertilizer price per short ton (per tn.). The price shows a notable correlation. As shown in the left panel of Figure 3, both nominal prices remain relatively low during the moderate period of 1982 to 2007, after which both prices increase sharply due to surge in the global commodity prices and economic recession.

Figure 3: Corn and phosphorus fertilizer price dynamics



Notes: Inflation-adjusted prices are adjusted using the Consumer Price Index (CPI) for all urban consumer (index 1983=100), with data sourced from the [Federal Reserve Bank of Minneapolis \(2024.04\)](#).

The right panel of Figure 3, which shows the inflation-adjusted prices, more clearly illustrates the changing dynamics. Before 2007, the inflation-adjusted prices of both corn and P fertilizer show a decreasing trend, reflecting a period of declining real prices that suggest a market characterized by an oversupply relative to earlier years. After 2007, this trend sharply reversed, with the corn and P fertilizer prices beginning to rise significantly, indicating a shift to a high-price regime. This rise aligns with the global increase in commodity prices and marks a distinct change in market dynamics. This information can support the rationale for implementing a two-regime MSDR model, effectively distinguishing between the earlier period of declining prices and the subsequent period of rapid price escalation.

Thus, Figure 3 suggests that the two-regime MSDR model, $r_t \in \{\text{moderate, high}\}$, is suitable for capturing the non-linear and regime-dependent nature of the dynamics underlying corn and P fertilizer prices. We use inflation-adjusted prices in the MSDR model to ensure that the analysis reflects real market dynamics undistorted by inflation. This enables the model to accurately identify different market regimes based on real economic changes rather than nominal price shifts. Tables 3 and 4 present the results of the MSDR model and the transition probabilities of the inflation-adjusted corn and P fertilizer prices, respectively. Table 3 demonstrates how the impact of current prices on future prices varies depending on whether the market is in a moderate or high regime. In the moderate regime, the current corn price at the time significantly influences future price, indicating price persistence. However, the current P fertilizer price exerts a statistically nonsignificant effect on the corn price. In contrast, during the high regime, the influence of the current corn price is nonsignificant, whereas the effect of the P fertilizer price on the corn price is statistically significant, suggesting

Table 3: Markov switching dynamics regression for corn and phosphorus fertilizer prices

	Corn ($\ln(P_{t+1}^Y)$)		Phosphorus fertilizer ($\ln(P_{t+1}^F)$)	
	Moderate	High	Moderate	High
$\ln(P_t^F)$	0.091 (0.186)	0.763*** (0.284)	0.947*** (0.151)	-1.347*** (0.251)
$\ln(P_t^Y)$	0.633*** (0.199)	0.280 (0.205)	-0.034 (0.097)	2.234*** (0.470)
Const.	-0.410	-3.408** (1.448)	0.275 (0.723)	11.866*** (1.862)
$(\alpha_{0,r_t}, \beta_{0,r_t})$				
Std Dev.		0.109 (0.014)		0.075 (0.009)
$(\sigma_{\epsilon,r_t}, \sigma_{v,r_t})$				
Log-likelihood		12.309		31.502
AIC		-0.207		-1.406

Notes: Robust standard errors are in parentheses. In the regression, constant standard deviation $\sigma^2 = \sigma_i^2 = \sigma_j^2$ is assumed for $r_t \in \{i, j\}$, $i \neq j$. *, **, and *** denote significance at the 10%, 5%, and 1% levels, respectively.

that input costs begin affecting corn prices more substantially.

For P fertilizer prices, the moderate regime reveals a strong dependence on its own current price, indicating that current prices are predictive of future prices under moderate conditions. The effect of the current corn price on the fertilizer price in this regime is nonsignificant. The high regime sees the dynamics change: The coefficient of the current P fertilizer price turns negative, signifying that increasing current prices may lead to reduced future prices, a reversal that can reflect unpredictable supply and demand dynamic under stress. Additionally, the influence of the corn price on the fertilizer price is significantly positive, showing that in a high regime, the price of corn can have an upward impact on P fertilizer prices, possibly due to increased production affecting the broader agricultural market. Table 4 shows, for example, that the corn price has a 71.1% likelihood of remaining at a moderate regime during the next period given that the process is moderate during the current period as well as a 28.9% likelihood of moving to a high regime.

Table 5 presents the results of the specification tests for the MSDR model in relation to the equality of the inflation-adjusted price coefficients across the moderate and high regimes. The tests are designed to determine whether the impact of prices in time t on future $t + 1$ prices differ significantly between the two regimes. The results of the tests on

Table 4: Transition probabilities of corn and phosphorus fertilizer prices

	Corn (p_{ij}^Y)		Phosphorus fertilizer (p_{ij}^F)	
	Moderate (t)	High (t)	Moderate (t)	High (t)
Moderate ($t + 1$)	0.711	0.370	0.966	0.207
High ($t + 1$)	0.289	0.630	0.034	0.793

Notes: State value of corn and phosphorus fertilizer prices, P^Y and P^F , for the moderate and high state are predicted and averaged from the price data and Markov switching dynamics regression results.
 $P_{\text{Moderate}}^Y = \1.498 , $P_{\text{High}}^Y = \$2.030$ per bu. and $P_{\text{Moderate}}^F = \177.328 , $P_{\text{High}}^F = \$433.547$ per tn.

Table 5: Statistical tests for coefficient equality across regime

	Switching in corn price	Switching in phosphorus fertilizer price
$H_0 : \alpha_{1,\text{morderate}} = \alpha_{1,\text{high}}$	3.83**	
$H_0 : \alpha_{2,\text{morderate}} = \alpha_{2,\text{high}}$	7.19***	
$H_0 : \beta_{1,\text{morderate}} = \beta_{1,\text{high}}$		28.34***
$H_0 : \beta_{2,\text{morderate}} = \beta_{2,\text{high}}$		21.32***

Notes: The results of the Wald test and values indicate the chi-squared statistic. *, **, and *** denote significance at the 10%, 5%, and 1% levels, respectively.

the equality of the corn price coefficient, $\alpha_{1,r_{t+1}}$, $\beta_{2,r_{t+1}}$, and the P fertilizer price coefficient, $\alpha_{2,r_{t+1}}$, $\beta_{1,r_{t+1}}$, across the regimes are highly significant. This strongly rejects the proportion of the equality hypothesis that coefficients are the same across regimes, suggesting that the dynamics underlying P fertilizer and corn prices differ depending on the regime characterizing the market. This also supports the notion that there are distinct regimes in the market with different price dynamics, again validating the use of the two-regime MSDR model to capture the differences in price changes over time.

4.2 Optimal Policy and Dynamics of Legacy Phosphorus

Figure 4 is composed of four graphs arranged in a two-by-two grid, each illustrating the optimal policy based on the bioavailability of legacy P, uncertainty, and the economic variables of the corn and P fertilizer prices. The horizontal axis measures legacy P bioavailability

(mg/dm³) within a range of 1 to 45mg/dm³.⁵ The vertical axis represents uncertainty, as measured by the coefficient of variation (CV) in L beliefs, from 1% to 50%.

As indicated in each graph, four levels of P fertilizer application are considered: no application (0 kg/ha), low application (50 kg/ha), medium application (100 kg/ha), and high application (150 kg/ha). Figure 4 illustrates that when uncertainty in legacy P bioavailability is high, farmers tend to apply more P fertilizer and are more likely to adopt soil sampling, due to their risk-averse nature. Soil sampling when legacy P is low is intended to precisely assess legacy P bioavailability and optimize fertilizer application. Soil sampling enables farmers to identify P deficiencies, enabling them to apply P fertilizer more effectively and efficiently, thus ensuring that crops have the necessary nutrients required for optimal growth. Furthermore, farmers adopt soil sampling more frequently when legacy P is scarce than when it is abundant to minimize costs and the reduction in crop yield due to P deficiency.

When the mean estimated legacy P bioavailability is relatively very low, farmers opt for point sampling instead of standard sampling. In this situation, farmers can make better-informed decisions on the optimal amount of P fertilizer needed to improve crop yield by obtaining precise information on the level of legacy P bioavailability. The preference for point sampling under these conditions reflects a strategic investment to reduce the uncertainty and risks associated with low legacy P and to optimize P fertilizer application to generate improved economic returns.

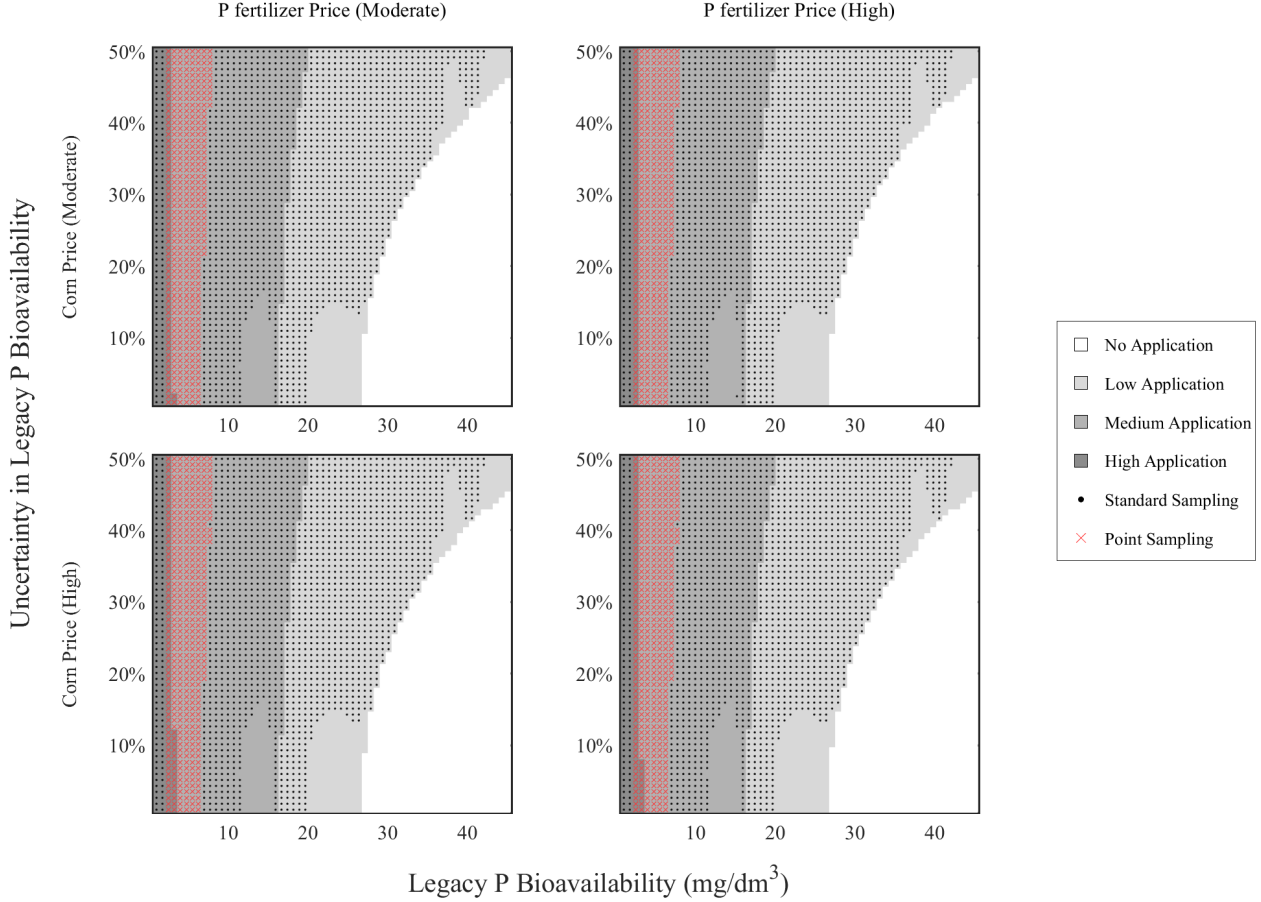
Next, Figure 5 presents the dynamics of the belief state in four different cases and the controlled dynamics of two belief state variables (1) legacy P bioavailability and (2) uncertainty in bioavailability (CV) over a 150-year period. Each of the two graphs in columns represents a different initial condition used for the 10,000 simulations: legacy P abundance and uncertainty.⁶

The 1st row displays the accumulation of legacy P bioavailability. Here, the range of possible legacy P bioavailability broadens as the simulation approaches the latter years. The average of the sample paths converges toward approximately 3.5mg/dm³. The 2nd row, which depict the uncertainty in legacy P bioavailability (CV), also reveal convergence toward low CV levels of approximately 2%.

⁵The range of legacy P bioavailability is determined by the critical level of soil P, that the probability of yield response to additional P fertilizer is not economically viable ([Gatiboni et al. 2021](#)). Based on the North Carolina research data, [Gatiboni et al. \(2021\)](#) found that soil with a P availability exceeding 35mg/dm³ exhibited relatively small response to fertilization. We extend the range to 45mg/dm³ to account for the variability in soil types and crop demand, thereby enable broader applicability of our finding.

⁶The initial price condition begins with a moderate corn price and moderate P fertilizer price. Other initial condition results are provided in the Appendix.

Figure 4: Optimal policy of P fertilizer application and soil sampling

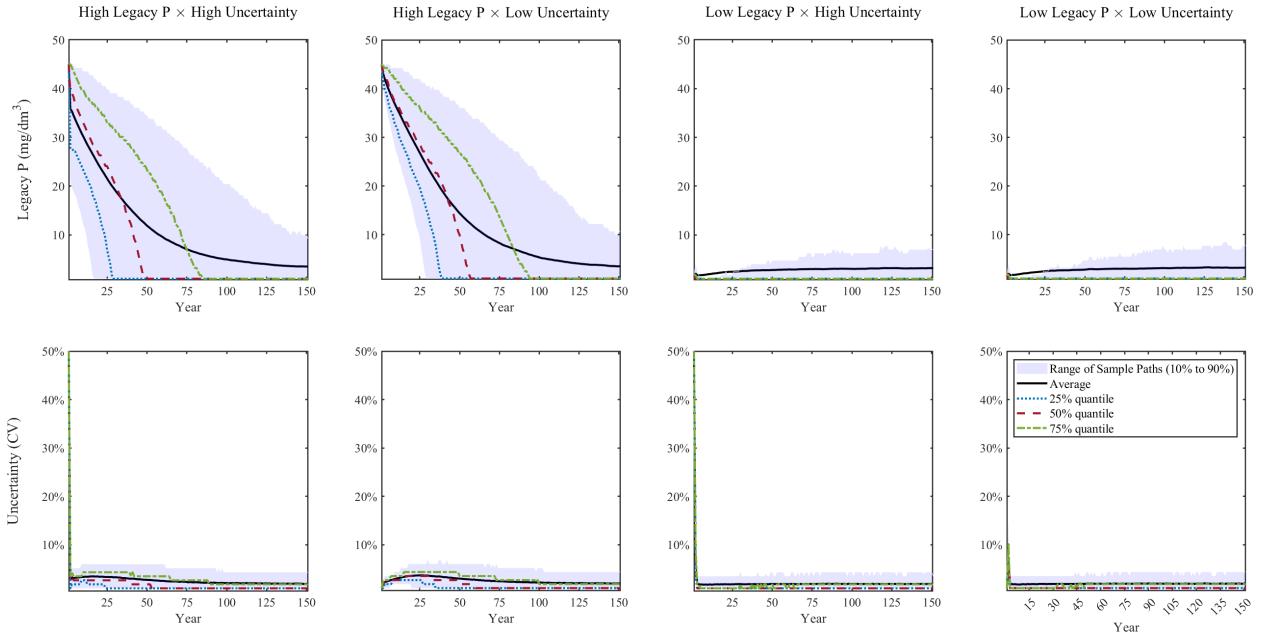


4.3 Risk Analysis: Epstein-Zin Preference

DP mapping is an efficient method for solving belief \times price MDP by breaking the optimization problem down into a sequence of subproblems. However, it assumes a risk-neutral decision-maker. To understand the effects of risk preferences on the legacy P management problem, we extended our MOMDP model by incorporating an Epstein-Zin preferences ([Epstein and Zin 1989](#)).

Since we have no data on farmer fertilizer decisions in this context that would have permitted on estimation of η and ψ , we chose the range of estimated parameters from the literature on environmental and agricultural studies listed in Table 6. What is more important for our analysis than specific values is the effect of high or low RA and EIS on model results. In the literature, the RA and EIS ranges are defined as $0.5 \leq \eta \leq 15$ and $0.1 \leq \psi \leq 3.3$, respectively. For our benchmark parameters, we choose multiple parameters across the ranges from which $\eta = (0.5, 5)$ and $\psi = (1.5, 3)$ were selected. In addition to benchmark parameters,

Figure 5: Dynamics of legacy P bioavailability and uncertainty



the risk-neutral condition, $\eta = 0$, and the perfectly elastic intertemporal substitution, $\psi = \infty$, are considered. When $\eta = 0$ and $\psi = \infty$, the problem is reduced to a standard DP problem seeking to maximize the expected NPV of profits.

Figure 6 shows how optimal policy changes with η and ψ . As η increased, indicating higher risk aversion, there is a noticeable shift toward higher P fertilizer application across all levels of bioavailability.⁷ This trend underscores the precautionary behavior adopted by risk-averse farmers who, facing uncertainty, prefer to ensure sufficient P fertilizer and legacy P levels for crop yield rather than risk potential yield losses. This decision is modulated by ψ modulates, with lower ψ suggesting a preference for less intertemporal fluctuation in profit. This is demonstrated by a propensity to immediately apply more P fertilizer rather than defer application and potentially affect future profits. The patterns of soil sampling are also contingent on η and ψ .

Under conditions of low legacy P bioavailability and high CV, soil sampling is increasingly adopted, especially as ψ increases. These results indicate that farmers are more willing to tolerate intertemporal fluctuation in payoff, strategically reducing fertilizer inputs and enhancing their sampling efforts to obtain precise information about legacy P levels. This tendency is particularly notable in the risk neutral condition ($\eta = 0$), where higher ψ leads to a significant shift toward decreased fertilizer use and increased soil sampling, with the aim

⁷Initial corn and P fertilizer price states are moderate. Other initial condition results are provided in the Appendix.

Table 6: Estimated value of risk aversion and elasticity of intertemporal substitution in literature

Literature		RA (η)	EIS (ψ)
Howitt et al. (2005)	California (US)	1.4	0.1
Cai and Lontzek (2019)		10	0.5, 1.5
Lybbert and McPeak (2012)	Chalbi (Keyna)	0.5 (OLS) 0.8 (IV)	0.7(OLS) 0.9(IV)
	Dukana (Keyna)	13.5 (OLS) 12.5 (IV)	2.8(OLS) 3.3(IV)
Daniel et al. (2019)		1.1-15	0.6-1.2

Notes: OLS and IV indicate Ordinary Least Squares regression and Instrumental variables estimation, respectively.

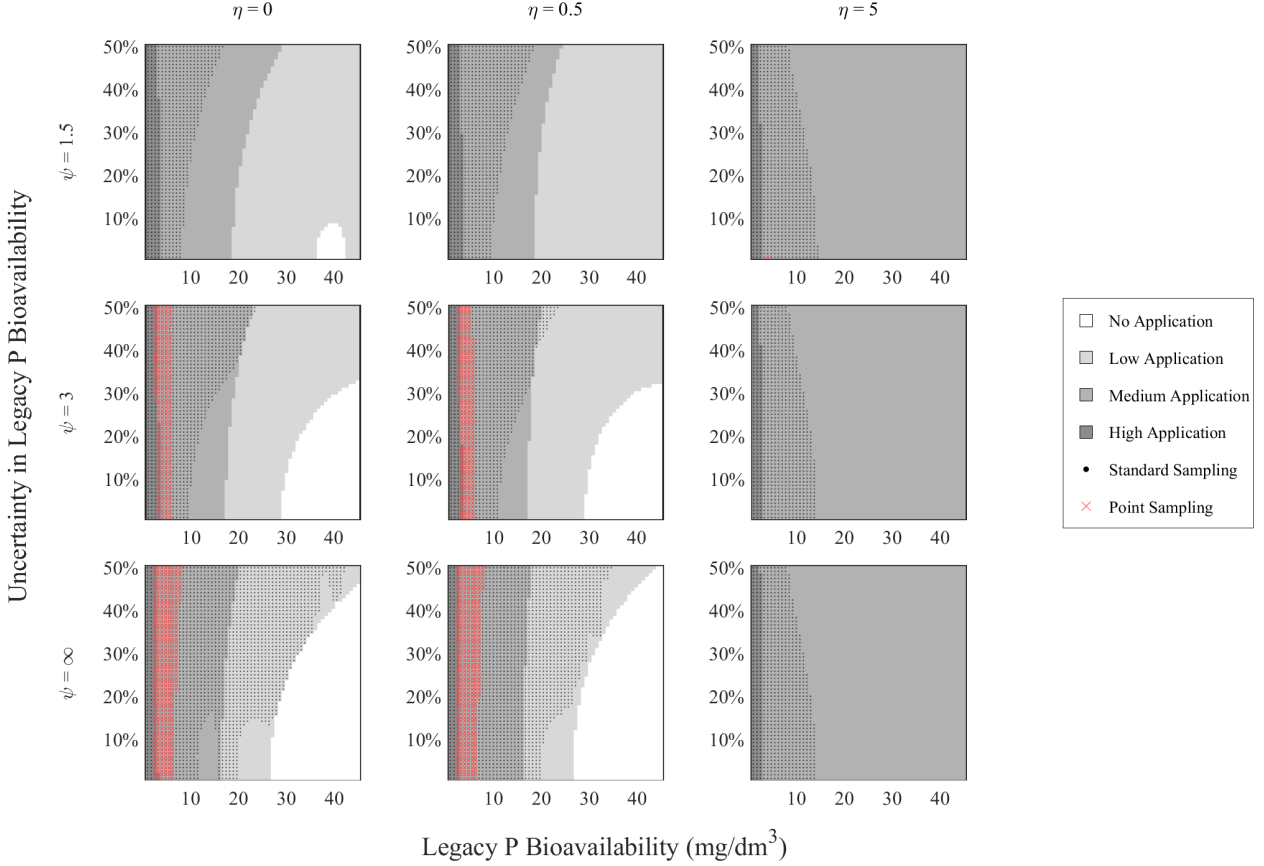
for more effective cost savings on fertilizers.

However, when farmers exhibit considerable risk aversion, their approach to managing soil sampling go through a notable shift, even as ψ increases. Despite a higher ψ suggesting a greater willingness to substitute profit across time, the dominant factor for these farmers is the minimization of immediate risk to their crop yields. This risk aversion is pronounced, and the typical response to increasing ψ is overpowered by the imperative to ensure current crop yields.

In this context, the use of soil sampling, which provides precise information on legacy P levels and can potentially lead to more efficient fertilizer use in the current time, is still favored. The figure indicates that farmers maintain soil sampling adoption alongside high P fertilizer application. With increased η , however, come a shift away from point sampling, despite its effectiveness in offering highly detailed information about legacy P levels. This preference shift can be attributed to cost consideration and operational efficiency. Standard sampling offers a more cost-effective solution by providing information necessary for making fertilizer application decisions without the high expense associated with the denser, more detailed data collection required by point sampling. For a highly risk-averse farmer, the information on cost-effectiveness provided by standard soil sampling outweighs the long-term efficiency gain derived from point soil sampling. This perspective is embedded in a preference for a certain profit today, rather than potentially more optimized but uncertain profits in the future.

Correspondingly, under conditions of high-risk aversion and increasing ψ , famers prioritize controls and information acquisition that afford them immediate risk mitigation benefits over

Figure 6: Epstein-Zin preferences and Optimal policy of P fertilizer application and soil sampling

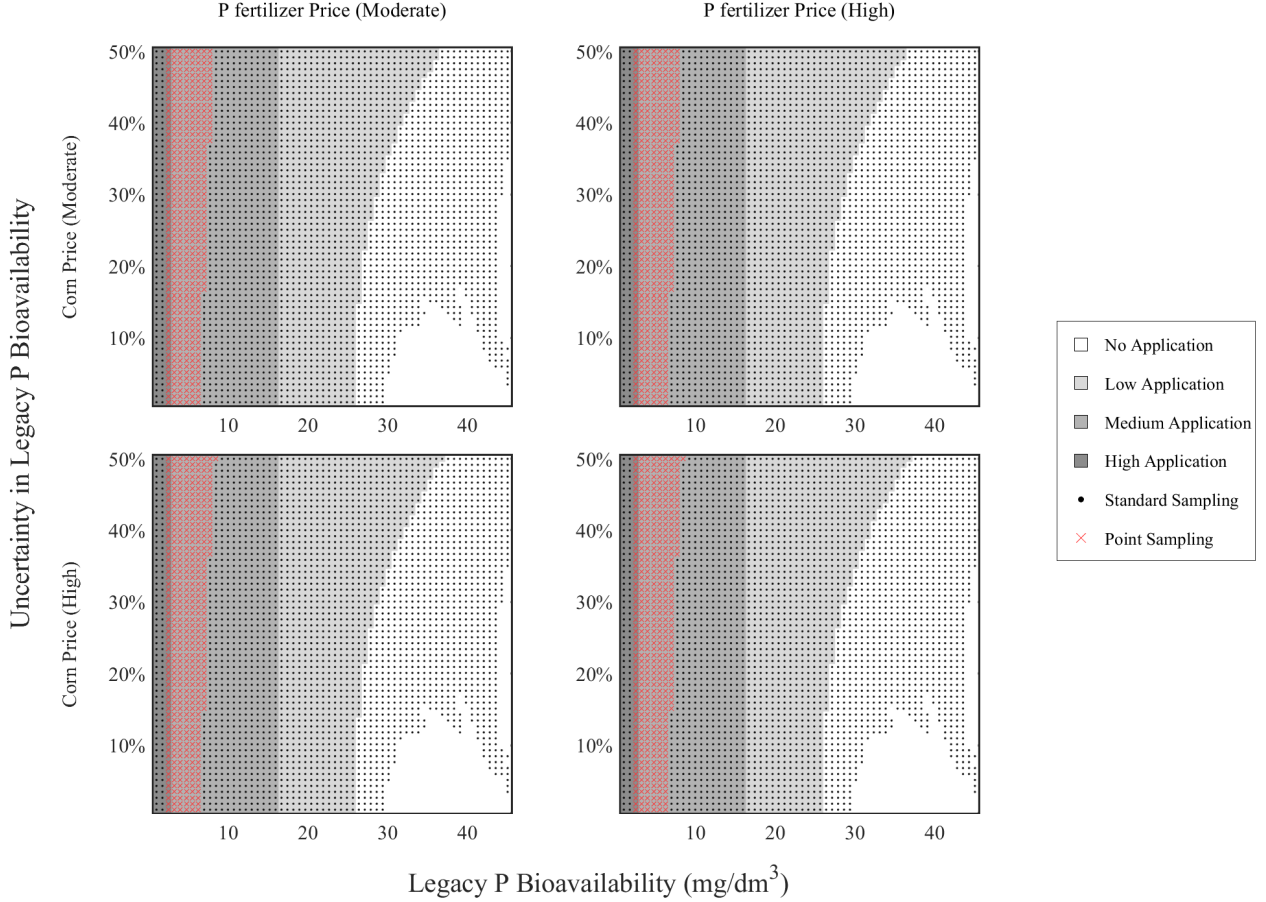


those that can improve efficiency but may introduce uncertainty. This behavior underlines an important point: When risk aversion is high, the risk reduction benefits of monitoring are dominated by the more powerful (and more expensive) risk management option of simply using more fertilizer to reduce yield risk.

5 Economic Sensitivity Analysis

A sensitivity analysis of economic conditions is also important for evaluating short-term productivity along with long-term agricultural sustainability when optimizing legacy P management using MOMDP. To understand the impact of varying economic conditions, we show the responses of the optimal policy to changes in the discount rate and exogenous shifts in P fertilizer prices (e.g. in response to a fertilizer tax).

Figure 7: Sensitivity analysis: 2% discount rate



5.1 Discount Rate

In previous economic studies on discount rates in agricultural and resource economics, the discount rates of farmers are relatively higher than those indicated in benefit-cost analyses recommended for federal programs ([Duquette et al. 2012](#)). For the scenario in our analysis, the baseline discount rate is adjusted to 2%, which is the 30-year real interest rate on treasury notes and bonds of specified maturities, thereby reflecting policymakers' perspectives ([Young 2023](#)).

Figure 7 depicts the sensitivity analysis of how the discount rate affects farmers' decisions regarding P fertilizer application and the adoption of soil sampling. As the discount rate decreases from 8% to 2%, the preference shifts toward ensuring long-term profitability. Thus, the farmers are less likely to apply P fertilizer and more likely to employ soil sampling. In particular, farmers implement more frequent soil sampling under greater uncertainty in legacy P bioavailability. These findings can be explained by two economic perspectives.

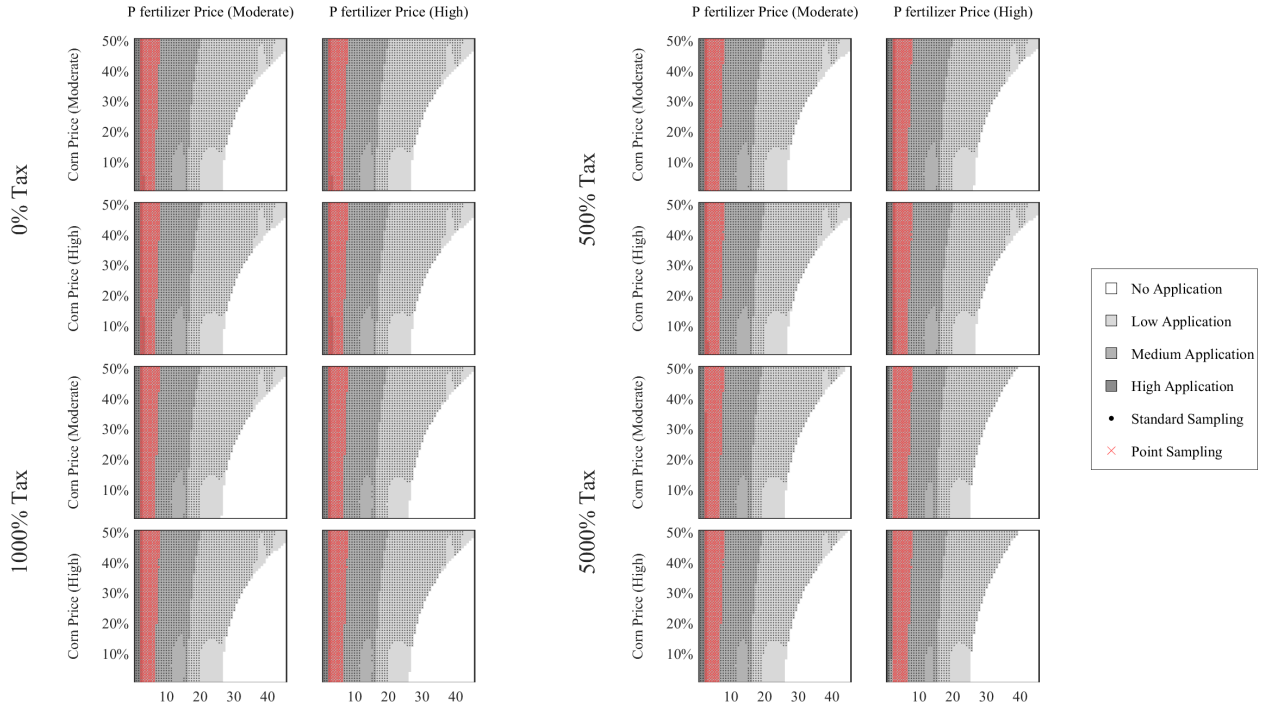
First, the option value of the investment decision on improved information, or the benefits of acquiring information from soil sampling before making a P fertilizer application decision varies considerably across the alternative discount rate scenarios and tremendously influences soil sampling choices. With a low discount rate, the option value of the information obtainable from soil sampling becomes more important. When the discount rate decreases and farmers more heavily weigh future payoffs in their decisions, they may attach greater value to the flexibility that the information provides. Second, this farmer behavior can be interpreted through precautionary saving. Farmers may save on future production costs by increasing investment in soil sampling, reducing their exposure to risks on future yield. This strategy resembles an investment in information capital, akin to how investors allocate resources to gather market information and secure long-term economic stability. By increasing soil sampling, farmers are effectively investing in a deeper understanding of legacy P levels. This strategic allocation of resources not only enhances their capacity for informed decision making but also prepares them to better handle the uncertainties of future P nutrient management. Such investments also pave the way for farmers to optimize their use of fertilizers, thus potentially reducing costs and increasing profitability over time.

5.2 Taxation on Phosphorus Fertilizer

Taxation on fertilizers to restrict chemical fertilization is a method to prevent water damage and this tool is incorporated by many states into their own environmental policies ([Osteen and Kuchler 1986](#), [Liang et al. 1998](#)). However, the effectiveness of taxation on agricultural chemicals in reducing chemical fertilization is unclear. [Liang et al. \(1998\)](#) examined the effect of taxation on P and nitrogen on fertilizer use through two tax schemes, namely uniform and differentiated taxes. Their study revealed that a 500% tax reduced only 8% of on-farm fertilizer usage but caused at least a 30% reduction in agricultural labor.

This section recounts our investigation of possible explanations for inelastic fertilizer demand. For the general sensitivity analysis, a uniform tax scheme is considered with tax rates of up to 0%, 500%, 1,000%, and 5,000%. The uniform tax scheme can be defined as follows: $P_{\text{tax}}^F = P^F (1 + \text{Tax Rate})$, where P^F is the producer price, and P_{tax}^F denotes the price of P fertilizer paid by farmers. Figure 8 represents how increased fiscal pressure on P fertilizer prices influences fertilizer application decisions within each taxation scenario. As taxation on P fertilizer intensified, farmers become more conservative and reduce P fertilizer application. However, despite the imposition of very high taxation rates on P fertilizer, no substantial decline in fertilizer application in farmland is observed. This trend can be attributed to several causes. Primarily, the demand for P fertilizer may be inelastic, with

Figure 8: Sensitivity analysis: taxation on phosphorus fertilizer



Notes: x-axis and y-axis indicate legacy P bioavailability and uncertainty in legacy P bioavailability, respectively.

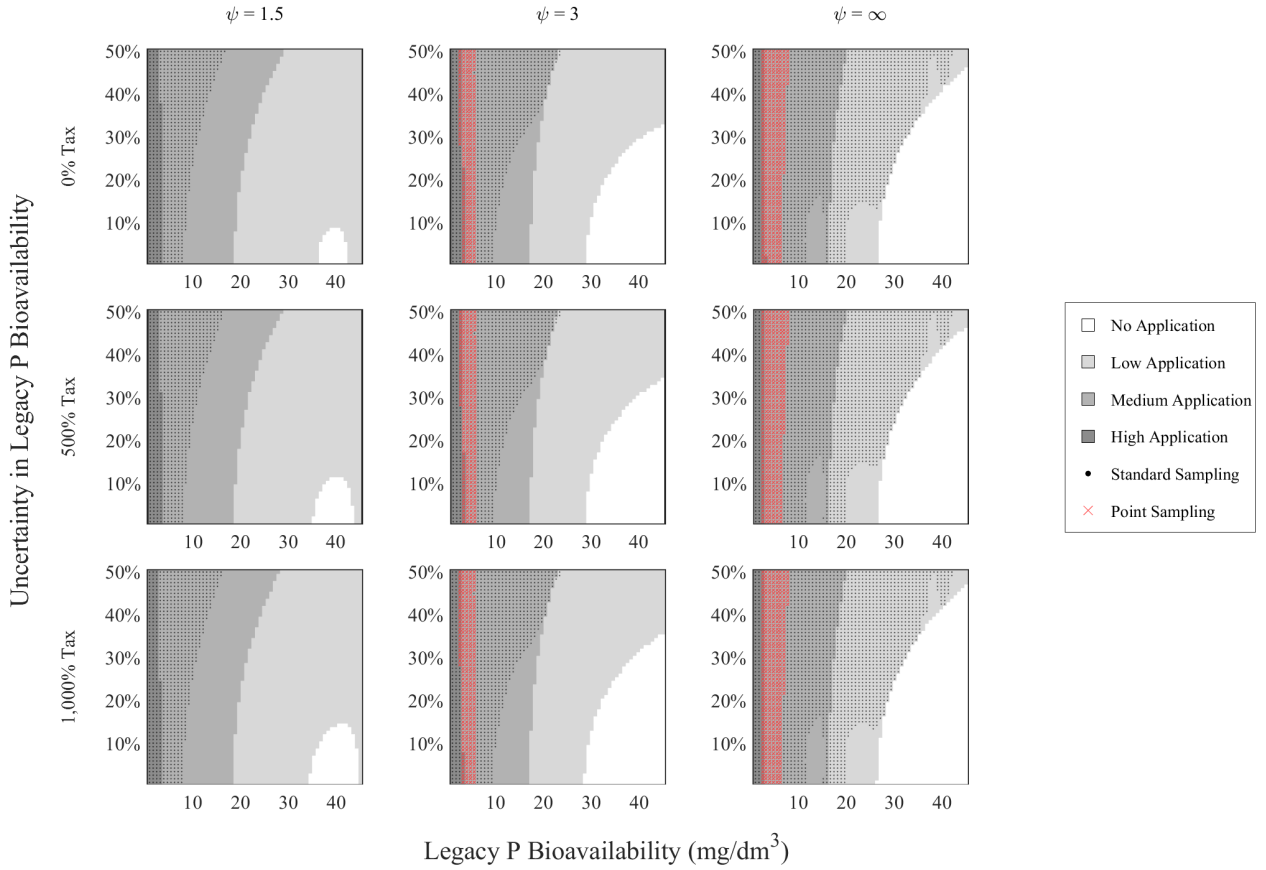
farmers considering it a necessary input for crop yield as it is an essential nutrient that cannot be replaced. In this particular cropping system, P fertilizer account for a relatively small share of the net revenue from total production costs on an annual basis, indicating room for farmers to absorb higher costs without forgoing positive profits.

Furthermore, farmers exhibit risk-averse behaviors, and may continue to apply fertilizer to minimize the risk of reduced yields due to P deficiencies, which can be financially more damaging than the cost of P fertilizer. Figure 9 illustrates that as tax rates on P fertilizer rise, risk neutral ($\eta = 0$) farmers do not proportionally reduce their use of P fertilizer.⁸ The persistence in P fertilizer application despite high taxation reflects farmers' prioritization of long-term yield assurance over immediate cost implications. Additionally, with the higher EIS reflecting tolerance of intertemporal fluctuations in payoffs, farmers are more inclined to sustain their fertilizer application to secure long-term crop yields despite rising taxation.

The utilization of soil sampling provides detailed information on legacy P bioavailability in the soil, thereby allowing farmers to determine the optimal amount of P fertilizer needed

⁸Initial corn and P fertilizer price states are moderate. Other initial condition results are provided in Appendix.

Figure 9: Risk neutral farmer responses to P fertilizer tax

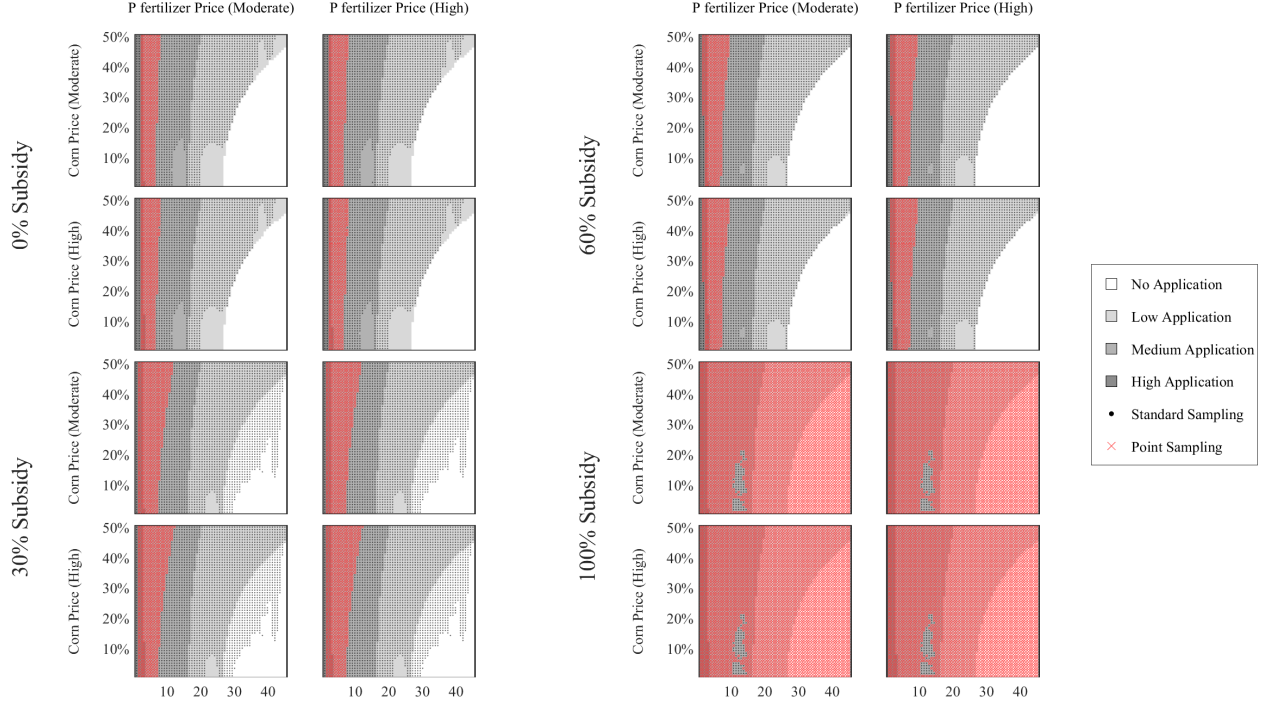


for their crop. With precise knowledge of existing soil nutrients, farmers can apply the exact amount of P fertilizer required. This makes it challenging to significantly reduce P fertilizer usage, even with high tax rates, because the application is tailored directly to a crop's needs. Additionally, the perspective of legacy P as a long-term saving measure for soil fertility may outweigh concerns over the immediate cost increases associated with taxation. In on-farm management, the use of P fertilizer ensures crop quality and yield, further motivating farmers to maintain or slightly adjust rather than significantly decrease P fertilizer applications in response to tax increases.

5.3 Subsidy on Soil Sampling

The adoption of soil sampling subsidies is a forward-looking agricultural policy instrument aimed at improving nutrient management practice among farmers. We study the potential impact of various levels of uniform subsidies on soil sampling rate, $c_s^{\text{subsidy}} = c_s(1 - \text{Subsidy Rate})$, at 0%, 30%, 60% and full (100%) subsidization. The results presented in Figure 10 reflect a

Figure 10: Sensitivity analysis: subsidy on soil sampling



Notes: x-axis and y-axis indicate legacy P bioavailability and uncertainty in legacy P bioavailability, respectively.

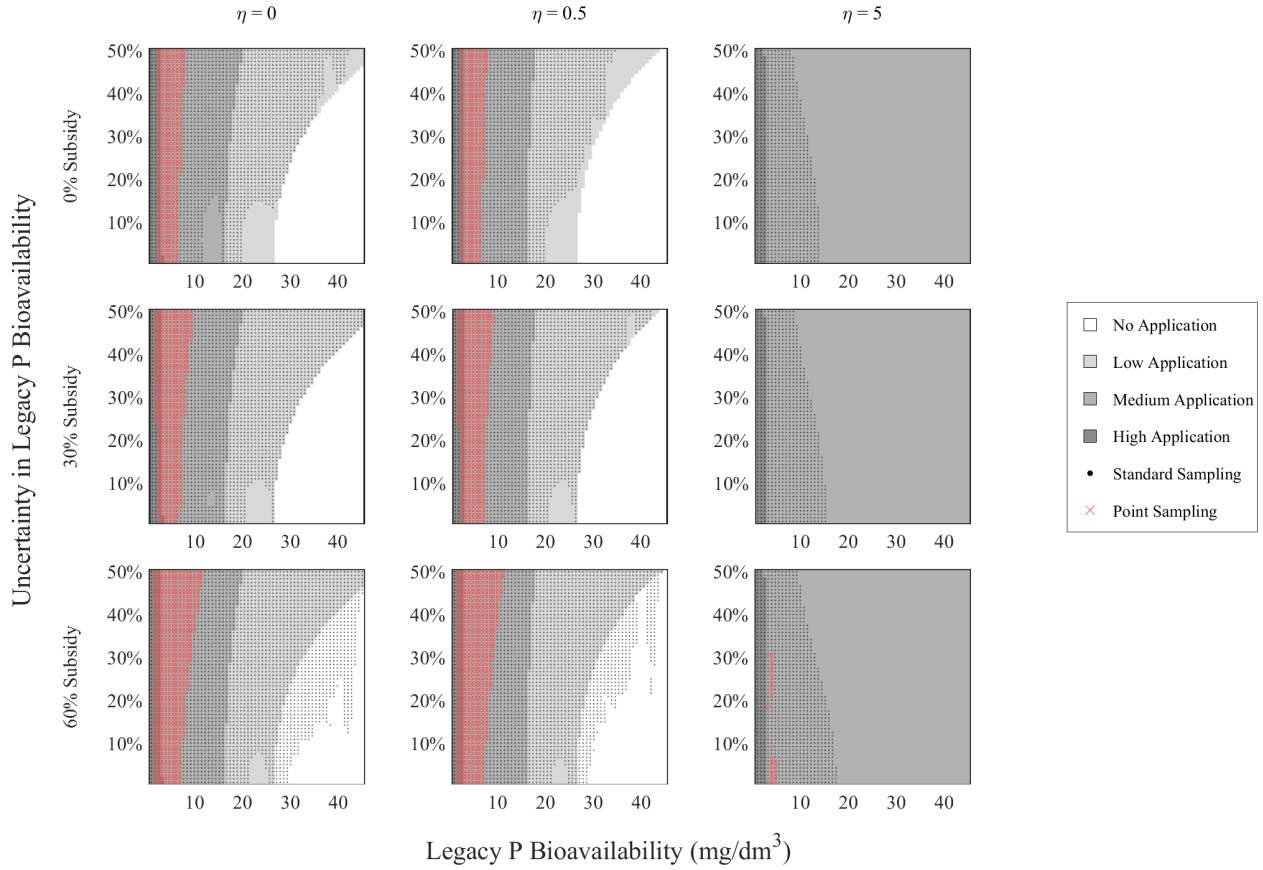
clear trend: As the subsidy rate increased, a corresponding rise occurs in the adoption of soil sampling, particularly point sampling with full subsidy.

This propensity toward greater soil sampling is indicative of a growing awareness and appreciation among farmers for the role of precise legacy P data in sustainable management. With subsidies easing financial loads, farmers are more inclined to assess the fertility of their soil, thus gaining valuable information that can inform their economic decisions. The increase in soil sampling, driven by subsidies, offers significant potential for long-term shifts in P management practices. As farmers become increasingly informed with detailed data derived on soil sampling, we may observe a refinement in P fertilizer application strategies, tailored to the precise needs of crops.

Figure 11 illustrates the impact of soil sampling subsidies on farmers with $\psi = \infty$, mapped against RA levels as denoted by $\eta = (0, 0.5, 5)$.⁹ The analysis shows that as η increased, farmers tend to apply P fertilizer at higher rates, regardless of the subsidy levels for soil sampling. Risk-averse farmers prioritize securing crop yields by applying P fertilizer,

⁹Initial corn and P fertilizer price states are moderate. Other initial condition results are provided in the Appendix.

Figure 11: Risk-averse farmer responses to soil sampling subsidy



even when subsidies are available to encourage soil sampling. This behavior underlines the precautionary actions taken by risk-averse individuals to mitigate the risk of yield loss due to insufficient nutrients. While financial incentives can encourage the adoption of soil sampling, they do not necessarily lead to a proportional decrease in fertilizer usage among risk-averse farmers. This suggests that although subsidies make soil sampling more accessible, the ingrained risk aversion and the perceived need to ensure crop yield stability drive continued high P fertilizer application rates. The results indicate that subsidies can effectively promote soil sampling, but that their influence on reducing fertilizer application is moderated by a farmer's risk preferences. High risk aversion diminishes the potential for subsidies to significantly alter fertilizer application practices.

The findings presented in Figures 10 and 11 have important implications for policy design. Policy makers should consider structuring subsidy programs to not only reduce the cost of soil sampling but also address the underlying risk preferences of farmers. Combining financial incentives with risk management education and tools can enhance the overall effectiveness of such programs. Providing farmers with education and resources to better understand and

manage risks associated with nutrient management can complement subsidy programs. By reducing the perceived risks related to crop yields, farmers may be more inclined to adjust their fertilizer application strategies.

Overall, while subsidies play a significant role in promoting soil sampling, addressing risk aversion through complementary measures is essential for achieving substantial change in fertilizer application practices. This comprehensive approach needs to be explored as a future project and can support sustainable P management, ensuring both agricultural productivity and environmental protection

6 Discussion

The overuse of P fertilizer in agriculture causes significant surface water pollution, necessitating policy solutions that encourage farmers to use less P fertilizer while minimizing economic losses in agricultural production. Because of the dynamic and stochastic nature of P accumulation in soil, combined with state uncertainty about legacy P stocks, this research adopts a model-based approach to disentangling these dynamics and their effects on the fertilizer demand and soil sampling behaviors of risk-averse farmers. We apply methods developed for the resource management problems involving the partial observability of resource stocks and advance these methods to include agent risk and intertemporal smoothing preferences through the Epstein-Zin preferences. Accordingly, we reveal that risk aversion among farmers significantly contributes to the price-inelastic demand for fertilizer and their reluctance to rely on estimated legacy P stocks, despite extensive efforts to promote the utilization of these resources.

The focus of this research is understanding behavioral change among farmers rather than the environmental damage caused by P runoff. This distinction is critical because our primary objective is to analyze how farmers respond to different economic and informational incentives concerning legacy P management. Our findings provide important insights into why farmers may not fully exploit legacy P stocks and how their risk aversion shapes their P fertilizer application decisions.

While the environmental impacts of P runoff, such as eutrophication and greenhouse gas emissions, are important, our study specifically targets farmer behavior. By understanding the decision-making processes of farmers, we can better design policies that are more likely to be adopted and effectively reduce the overconsumption of P fertilizer. Behavioral focus advances the creation of more practical and applicable solutions tailored to the needs and preferences of farmers, ultimately leading to more sustainable agricultural practice. This focus on farmer behavior can be extended in future research to incorporate environmental factors more explicitly. For instance, expanding the model to consider the environmental and

climate change implications of P management can provide a more comprehensive grasp of the overall impact of agricultural practices. Future studies can integrate spatial variability and explore interactions between farmland and adjacent areas, thus offering deeper insight into the collective economic and environmental outcomes of P fertilizer and soil sampling decisions.

Future research can also consider the multiple agents involved in the optimal management of the legacy P problem with additional areas. Currently, the environmental and resource economics literature using POMDP or MMDP generally explores single agents in their models. Some researchers examine multiple agents, but they construct separate problems for each agent and disregard the interaction between the control exercised by each agent and the unobservable state problem. However, in a collective study of legacy P management, there will be multiple agents, in addition to farmers, that have their own observations and beliefs about the environmental state, which may also include beliefs about other agents' actions and strategies. By incorporating inter-agent dynamics into our POMDP model ([Emery-Montemerlo et al. 2004](#)), the POMDP may be constructed and extended as a 'Partially Observable Stochastic Game' (POSG) to solve for the optimal policy among multiple, competitive, or cooperative, agents' profits ([Hansen et al. 2004](#)).

This study demonstrates the significant influence of risk aversion on farmer behavior, highlighting the need for policies that only provide economic incentives but also address the underlying risk preferences of farmers. Our research centers on farmer related aspects of decision-making regarding P fertilizer application and soil sampling, laying the groundwork for future explorations that integrate environmental impacts and multi-agent dynamics, farmer associated factors, and government initiatives, offering an exhaustive approach to sustainable agricultural practices.

References

- ARROW, K., P. DASGUPTA, L. GOULDER, G. DAILY, P. EHRLICH, G. HEAL, S. LEVIN, K.-G. MÄLER, S. SCHNEIDER, D. STARRETT, AND B. WALKER (2018): “Are we consuming too much?” *Journal of Economic Perspectives*, 11(1), 17.
- ARULAMPALAM, M. S., S. MASKELL, N. GORDON, AND T. CLAPP (2002): “A tutorial on particle filters for online nonlinear/non-Gaussian Bayesian tracking,” *IEEE Transactions on signal processing*, 50(2), 174–188.
- AUSTIN, R., L. GATIBONI, AND J. HAVLIN (2020): “Soil sampling strategies for site-specific field management,” *NC State Extension AG-439-36*.
- CAI, Y. AND T. S. LONTZEK (2019): “The social cost of carbon with economic and climate risks,” *Journal of Political Economy*, 127(6), 2684–2734.
- CHADÈS, I., T. G. MARTIN, S. NICOL, M. A. BURGMAN, H. P. POSSINGHAM, AND Y. M. BUCKLEY (2011): “General rules for managing and surveying networks of pests, diseases, and endangered species,” *Proceedings of the National Academy of Sciences*, 108(20), 8323–8328.
- CHEN, L. (2022): “Essays on the Economics of Soil Health Practices,” *North Carolina State University*.
- CLARK, C. W. (2010): “General rules for managing and surveying networks of pests, diseases, and endangered species,” *Mathematical Bioeconomics: The Mathematics of Conservation*. Wiley.
- CONLEY, D. J., H. W. PAERL, R. W. HOWARTH, D. F. BOESCH, S. P. SEITZINGER, K. E. HAVENS, C. LANCELOT, AND G. E. LIKENS (2009): “Controlling eutrophication: Nitrogen and phosphorus,” *Science*, 323(5917), 1014–1015.
- CZAJKOWSKI, M. AND W. BUDZIŃSKI (2019): “Simulation error in maximum likelihood estimation of discrete choice models,” *Journal of Choice Modelling*, 31, 73–85.
- DANIEL, K. D., R. B. LITTERMAN, AND G. WAGNER (2019): “Declining CO₂ price paths,” *Proceedings of the National Academy of Sciences*, 116(42), 20886–20891.
- DE FREITAS, N. (2001): “Sequential Monte Carlo methods in practice (Vol. 1, No. 2, p. 2),” *A. Doucet, & N. J. Gordon (Eds.). New York: Springer*.
- DENBALY, M. AND H. VROOMEN (1993): “Dynamic fertilizer nutrient demands for corn: A cointegrated and error-correcting system. American Journal of Agricultural Economics,” *American Journal of Agricultural Economics*, 75(1), 203–209.
- DOWNING, J. A., S. POLASKY, S. M. OLMSTEAD, AND S. C. NEWBOLD (2021): “Protecting local water quality has global benefits,” *Nature Communications*, 12(1), 2709.
- DUQUETTE, E., N. HIGGINS, AND J. HOROWITZ (2012): “Farmer discount rates: Experimental evidence,” *American Journal of Agricultural Economics*, 94(2), 451–456.
- EKHOLM, P., E. TURTOLA, J. GRÖNROOS, P. SEURI, AND K. YLIVAINIO (2005): “Phosphorus

- loss from different farming systems estimated from soil surface phosphorus balance,” *Agriculture, Ecosystems and Environment*, 110(3-4), 266–278.
- EMERY-MONTEMERLO, R., G. GORDON, J. SCHNEIDER, AND S. THRUN (2004): “Approximate solutions for partially observable stochastic games with common payoffs,” *Proceedings of the Third International Joint Conference on Autonomous Agents and Multiagent Systems*.
- EPSTEIN, L. G. AND ZIN (1991): “Substitution, risk aversion, and the temporal behavior of consumption and asset returns: An empirical analysis,” *Journal of Political Economy*, 99(2), 261–286.
- EPSTEIN, L. G. AND S. E. ZIN (1989): “Substitution, risk aversion, and the temporal behavior of consumption and asset returns: A theoretical framework,” *Econometrica*, 57(4), 937.
- FACKLER, P. AND K. PACIFICI (2014): “Addressing structural and observational uncertainty in resource management,” *Journal of Environmental Management*, 133, 27–36.
- FACKLER, P. L. (2014): “Structural and observational uncertainty in environmental and natural resource management,” *International Review of Environmental and Resource Economics*, 7(2), 109–139.
- FAN, X., M. I. GÈMEZ, S. S. ATALLAH, AND J. M. CONRAD (2020): “A Bayesian state-space approach for invasive species management: the case of spotted wing drosophila,” *American Journal of Agricultural Economics*, 102(4), 1227–1244.
- FEDERAL RESERVE BANK OF MINNEAPOLIS (2024.04): “Consumer Price Index, 1913-,” <https://www.minneapolisfed.org/about-us/monetary-policy/inflation-calculator/consumer-price-index-1913->.
- GATIBONI, L., D. OSMOND, AND D. HARDY (2021): “Careful Soil Sampling – The Key to Reliable Soil Test Information,” *NC State Extension AG-439-90*.
- (2022): “Changes in the Phosphorus Fertilizer Recommendations for Corn, Soybean, and Small Grains in North Carolina,” *NC State Extension AG-439-30*.
- GILBERT, R. J. (1979): “Optimal depletion of an uncertain stock,” *The Review of Economic Studies*, 46(1), 47.
- GOETZ, R. U. AND D. ZILBERMAN (2000): “The dynamics of spatial pollution: The case of phosphorus runoff from agricultural land,” *Journal of Economic Dynamics and Control*, 24(1), 143–163.
- HAIGHT, R. G. AND S. POLASKY (2010): “Optimal control of an invasive species with imperfect information about the level of infestation,” *Resource and Energy Economics*, 32(4), 519–533.
- HAMILTON, J. D. (1989): “A new approach to the economic analysis of nonstationary time series and the business cycle,” *Econometrica*, 57(2), 357.
- HANSEN, E. A., D. S. BERNSTEIN, AND S. ZILBERSTEIN (2004): “Dynamic Programming for Partially Observable Stochastic Games,” *American Association for Artificial Intelligence*.

- HOWITT, R. E., S. MSANGI, A. REYNAUD, AND K. C. KNAPP (2005): “Estimating intertemporal preferences for Natural Resource Allocation,” *American Journal of Agricultural Economics*, 87(4), 969–983.
- IHO, A. AND M. LAUKKANEN (2012): “Precision phosphorus management and agricultural phosphorus loading,” *Ecological Economics*, 77, 91–102.
- INNES, R. (2000): “The economics of Livestock Waste and its regulation,” *American Journal of Agricultural Economics*, 82(1), 97–117.
- KLING, D. M., J. N. SANCHIRICO, AND P. L. FACKLER (2017): “Optimal Monitoring and control under state uncertainty: Application to lionfish management,” *Journal of Environmental Economics and Management*, 84, 223–245.
- KOVACS, D. L., W. LI, N. FUKUTA, AND T. WATANABE (2012): “Mixed Observability Markov decision processes for overall network performance optimization in Wireless Sensor Networks,” *2012 IEEE 26th International Conference on Advanced Information Networking and Applications*.
- LAKE ERIE LAMP (2011): “Lake Erie Binational Nutrient Management Strategy: Protecting Lake Erie by Managing Phosphorus,” *Prepared by the Lake Erie LaMP Work Group Nutrient Management Task Group*.
- LIANG, C. L. K., S. B. LOVEJOY, AND J. G. LEE (1998): ““Green Taxes”: Impacts On National Income, Social Welfare, And Environmental Quality,” *Working Paper*.
- LIVINGSTON, M., M. J. ROBERTS, AND Y. ZHANG (2015): “Optimal sequential plantings of corn and soybeans under price uncertainty,” *American Journal of Agricultural Economics*, 97(3), 855–878.
- LÖTJÖNEN, S., E. TEMMES, AND M. OLLIKAINEN (2020): “Dairy farm management when nutrient runoff and climate emissions count,” *American Journal of Agricultural Economics*, 102(3), 960–981.
- LOURY, G. C. (1978): “The optimal exploitation of an unknown reserve,” *The Review of Economic Studies*, 45(3), 621–638.
- LYBBERT, T. J. AND J. MCPPEAK (2012): “Risk and intertemporal substitution: Livestock portfolios and off-take among Kenyan pastoralists,” *Journal of Development Economics*, 97(2), 415–426.
- MACLACHLAN, M. J., M. R. SPRINGBORN, AND P. L. FACKLER (2017): “Learning about a moving target in resource management: optimal Bayesian disease control,” *Journal of Environmental Economics and Management*, 99(1), 140–161.
- MELBOURNE, B. A. AND A. HASTINGS (2008): “Extinction risk depends strongly on factors contributing to stochasticity,” *Nature*, 454(7200), 100–103.
- MORALES, N. A., L. GATIBONI, D. OSMOND, R. VANN, S. KULESZA, C. CROZIER, AND D. HARDY (2023): “Critical soil test values of phosphorus and potassium for soybean and corn in three long-term trials in North Carolina,” *Soil Science Society of America Journal*, 87(2), 278–290.

- MYYRÄ, S., K. PIETOLA, AND M. YLI-HALLA (2007): “Exploring long-term land improvements under land tenure insecurity,” *Agricultural Systems*, 92(1-3), 63–75.
- OSTEEN, C. AND F. KUCHLER (1986): “Potential Bans of Corn and Soybean Pesticides: Economic Implications for Farmers and Consumers. AER-546,” *Economics Research Service*, U.S. Department of Agriculture.
- PAUDEL, J. AND C. L. CRAGO (2020): “Environmental externalities from agriculture: Evidence from water quality in the United States,” *American Journal of Agricultural Economics*, 103(1), 185–210.
- RABOTYAGOV, S. S., C. L. KLING, P. W. GASSMAN, N. N. RABALAIS, , AND R. E. TURNER (2014): “The economics of dead zones: Causes, impacts, policy challenges, and a model of the Gulf of Mexico hypoxic zone,” *Review of Environmental Economics and Policy*, 8, 58–79.
- RINGEVAL, B., J. DEMAY, D. S. GOLL, X. HE, Y. P. WANG, E. HOU, ..., AND S. PELLERIN (2018): “A global dataset on phosphorus in agricultural soils. Scientific Data,” *Scientific Data*, 11(1), 17.
- ROUT, T. M., J. L. MOORE, AND M. A. McCARTHY (2014): “Prevent, search or destroy? A partially observable model for invasive species management,” *Journal of Applied Ecology*, 51(3), 804–813.
- SATTARI, S. Z., A. F. BOUWMAN, K. E. GILLER, AND M. K. VAN ITTERSUM (2012): “Residual soil phosphorus as the missing piece in the global phosphorus crisis puzzle,” *Proceedings of the National Academy of Sciences*, 109(16), 6348–6353.
- SCHNITKEY, G. D. AND M. J. MIRANDA (1993): “The Impact of Pollution Controls on Livestock-Crop Producers,” *Journal of Agricultural and Resource Economics*, 18(1), 25–36.
- SIMS, C., D. FINNOFF, A. HASTINGS, AND J. HOCHARD (2017): “Listing and delisting thresholds under the Endangered Species Act,” *American Journal of Agricultural Economics*, 99(3), 549–570.
- SLOGGY, M. R., D. M. KLING, AND A. J. PLANTINGA (2020): “Measure twice, cut once: Optimal Inventory and harvest under volume uncertainty and Stochastic Price Dynamics,” *Journal of Environmental Economics and Management*, 103, 102357.
- SPRINGBORN, M. AND J. N. SANCHIRICO (2013): “A density projection approach for non-trivial information dynamics: Adaptive management of stochastic natural resources,” *Journal of Environmental Economics and Management*, 66(3), 609–624.
- TOMBERLIN, D. AND T. ISH (2007): “When is logging road erosion worth monitoring. In Proceedings of the International Mountain Logging and 13th Pacific Northwest Skyline Symposium (pp. 239–244),” *Oregon State University, College of Forestry Corvallis Oregon*.
- UC DAVIS ANALYTICAL LAB (2024): “Exploring long-term land improvements under land tenure insecurity,” *Current Price. UC David. <https://anlab.ucdavis.edu/Prices>*.
- US EPA (1995): “In National Nutrient Assessment Workshop: Proceedings, December 4-6,” *United States Environmental Protection Agency, Washington, D.C.*

- USDA (2020): “Legacy Phosphorus Project,” *United States Department of Agriculture*.
- USDA (2024a): “Fertilizer Use and Price,” *United States Department of Agriculture*, <https://www.ers.usda.gov/data-products/fertilizer-use-and-price/>.
- (2024b): “U.S. Bioenergy Statistics,” *United States Department of Agriculture*, <https://www.ers.usda.gov/data-products/u-s-bioenergy-statistics/>.
- WHITE, B. (2005): “An economic analysis of Ecological Monitoring,” *Ecological Modelling*, 189(3-4), 241–250.
- WIRONEN, M. B., E. M. BENNETT, AND J. D. ERICKSON (2018): “Phosphorus flows and legacy accumulation in an animal-dominated agricultural region from 1925 to 2012,” *Global Environmental Change*, 50, 88–99.
- YOUNG, D. S. (2023): “Memorandum for Heads of Executive Departments and Establishments: 2023 Discount Rates for OMB Circular No. A-94,” *Office of the Management and Budget*.
- ZHOU, E., M. C. FU, AND S. I. MARCUS (2010): “Solving continuous-state POMDPs via density projection,” *IEEE Transactions on Automatic Control*, 55(5), 1101–1116.
- ZOU, T., X. ZHANG, AND E. A. DAVIDSON (2022): “Global trends of cropland phosphorus use and sustainability challenges,” *Nature*, 611(7934), 81–87.

Appendix

A Methodology and Algorithms

This appendix offers further details and elaborates on the methodology described in the main paper. It begins with the foundation of our methodology and concludes by presenting supplementary figures.

A.1 Detailed formulation of the Dynamic Programming Model

The Bellman equation for the recursive expected utility function (equation 8) can be detailed as:

$$V(b_t, P_t^Y, P_t^F) = \max_{F,s} \iint \pi(L_t, F_t, P_{t+1}^Y, P_t^F, s_t) b_t f(P_{t+1}^Y | P_t^Y, P_t^F) dP_{t+1}^Y dL_t \\ + \beta \iiint p(P_{t+1}^F | P_t^F) p(P_{t+1}^Y | P_t^Y) p(O_{t+1}^l | b_{t+1}, P_{t+1}^Y, P_{t+1}^F) V(b_{t+1}, P_{t+1}^Y, P_{t+1}^F) dO_{t+1}^l dP_{t+1}^Y dP_{t+1}^F, \quad (\text{A1})$$

and given Epstein-Zin preferences, the equation 10 can be further detailed as:

$$V_{EZ}(b_t, P_t^Y, P_t^F) = \max_{F,s} \left[\left(\iint \pi(L_t, F_t, P_{t+1}^Y, P_t^F, s_t)^{1-\eta} b_t f(P_{t+1}^Y | P_t^Y, P_t^F) dP_{t+1}^Y dL_t \right)^{\frac{1-\psi^{-1}}{1-\eta}} \right. \\ \left. + \beta \left(\iiint p(P_{t+1}^F | P_t^F) p(P_{t+1}^Y | P_t^Y) p(O_{t+1}^l | b_{t+1}, P_{t+1}^Y, P_{t+1}^F) V_{EZ}(b_{t+1}, P_{t+1}^Y, P_{t+1}^F)^{1-\eta} dO_{t+1}^l dP_{t+1}^Y dP_{t+1}^F \right)^{\frac{1-\psi^{-1}}{1-\eta}} \right]^{\frac{1}{1-\psi^{-1}}}, \quad (\text{A2})$$

under state variables, b_t , P_t^Y , P_t^F at time t .

A.2 Solution Methods of Projected Belief

The projected belief MDP is a low-dimensional, continuous state MDP (Zhou et al. 2010). To facilitate the value iteration, we first convert the projected belief MDP into a discrete state MDP.¹⁰ This conversion involves discretizing the space of natural parameters θ in the exponential distribution $f(\cdot | \theta)$ (Zhou et al. 2010). In this paper, we employ the log normal distribution to define legacy P bioavailability μ_L and uncertainty in legacy P bioavailability as CV, $CV_L = \sigma_L / \mu_L$ with a parameter set $\delta = \{\mu_L, CV_L\}$. Hence, we discretize θ by calculating the univariate log normal parameters μ and σ that $\theta = \{\mu, \sigma\}$ where $\sigma > 0$ from the δ (Kling

¹⁰The discretization and estimation methods are adopted from Zhou et al. 2010 and Kling et al. 2017.

et al. 2017). The calculation of μ and σ is follows:

$$\mu = \ln \left(\frac{\mu_L^2}{\sqrt{\mu_L^2 + \sigma_L^2}} \right), \quad \sigma^2 = \ln \left(1 + \frac{\sigma_L^2}{\mu_L^2} \right). \quad (\text{A3})$$

For the estimation in discretized space, μ_L and σ_L are discretized into a 60×1 vector. A 60×60 mesh grid $\{\delta_i\}_{i=1}^N = G$ is then calculated, incorporating all grid points $\delta_i = \{\mu_{L,i}, \sigma_{L,i}\}$ where $CV_{L,i} = \sigma_{L,i}/\mu_{L,i}$. Within this discretized state space δ_i , the crop profit function is evaluated as the expected value of δ_i , in associated with controls F , s and prices P^Y , P^F . By defining the transition probability as $\tilde{p}(\delta_i, F, s)(\delta_j)$, representing the probability to transitioning from δ_i to δ_j , the discretized belief MDP for equation 10 is formulated as:¹¹

$$\begin{aligned} \tilde{V}(\delta_i, P^Y, P^F) &= \max_{F,s} \tilde{\pi}(\delta_i, F, P^Y, P^F, s) \\ &+ \beta \sum_{j=1}^{P^{F'}} \sum_{i=1}^{P^{Y'}} \sum_{j=1}^N p(P^{F'}|P^F) p(P^{Y'}|P^Y) \tilde{p}(\delta_i, F, s)(\delta_j) \tilde{V}(\delta_j, P^{Y'}, P^{F'}), \end{aligned} \quad (\text{A4})$$

where $p(P^{F'}|P^F)$ and $p(P^{Y'}|P^Y)$ denote the discretized transition probability of corn and P fertilizer prices, estimated from the MSDR model.

The profit function $\tilde{\pi}(\delta_i, F, P^Y, P^F, s)$ and transition probability $\tilde{p}(\delta_i, F, s)(\delta_j)$ associated with controls F and s can be estimated by using Monte-Carlo simulation, as follows (Zhou et al. 2010):

Algorithm 1. Estimation of Crop Profit Function

Input: $\delta_i, P^Y, P^F, F, s, \omega^2$

Output: $\tilde{\pi}(\delta_i, F, P^Y, P^F, s)$

Step 1. Sampling:

$$\mathbf{L} = f^{-1}(\omega^2 | \theta_i) \quad \text{where } \mathbf{L} = \{L_1, L_2, \dots, L_Z\}$$

Step 2. Estimation:

$$\tilde{\pi}(\delta_i, F, P^Y, P^F, s) = \frac{1}{Z} \sum_{j=1}^Z \sum_{P^{Y'}} \pi(L_j, F, P^{Y'}, P^F, s) f(P^{Y'}|P^Y, P^F)$$

Source: Zhou et al. (2010)

ω^k is the set of Sobol points $\omega^k = \{\omega_1^k, \omega_2^k, \dots, \omega_Z^k\}$ that derived from Sobol sequence. For the estimation of crop profit function and transition probability, we use the three-dimensional

¹¹In price dynamics, the $t + 1$ state is represented by ' notation.

($k = 3$) Sobol points ω^k that includes $Z = 10,000$ points. In the draw process, the Sobol draw omits an initial 1,000 points, then select every 101st point thereafter. We also apply a random linear scramble along with a random digit shift. In the estimation of log-likelihood function, Sobol draw is efficient methods. To achieve the same precision level of 1,000 Sobol draws in the estimation of log-likelihood function value, the estimation requires the 1,661 Haltom draws, 4,155 Modified Latin Hyper Cube Sampling draws or 9,987 pseudo-random draws ([Czajkowski and Budziński 2019](#)). With a five-dimensional Sobol draw, the desired precision level requires at least 2,100 points ([Czajkowski and Budziński 2019](#)), and we choose the number of points to 10,000 to increase the precision level.

Estimation of transition probability $\tilde{p}(\delta_i, F, s)(\delta_j)$ is follows:

Algorithm 2. Estimation of transition probability

Input: $\delta_i, P^Y, P^F, F, s, \omega^1, \omega^2, \omega^3$

Output: $\tilde{p}(\delta_i, F, s)(\delta_j)$

Step 1. Sampling:

$$\mathbf{L} = f^{-1}(\omega^2 | \theta_i) \quad \text{where } \mathbf{L} = \{L_1, L_2, \dots, L_Z\}$$

Step 2. Compute $\tilde{\mathbf{L}}$ by propagation of \mathbf{L} according to the dynamics of legacy P (equation 1) using controls F and s , and carry-over parameter ρ that is generated using ω^1 .

Step 3. Compute $O_1, O_2, O_3, \dots, O_Z$ from $\tilde{\mathbf{L}} = \{\tilde{L}_1, \tilde{L}_2, \tilde{L}_3, \dots, \tilde{L}_Z\}$ using equation 5 and observation error $\{\lambda_i^l\}_{i=1}^Z$ that is generated by ω^3 , where l is determined by the controls F and s .

Step 4. For each $O_k, k = 1, 2, \dots, Z$, compute the updated belief state

$$\tilde{b}_k = \sum_{i=1}^Z \tau_i^k \phi(L - \tilde{L}_i),$$

where ϕ is the Kronecker delta product function and

$$\tau_i^k = \frac{p(O_k | \tilde{L}_i, F, s)}{\sum_{i=1}^Z p(O_k | \tilde{L}_i, F, s)}$$

Step 5. For $k = 1, 2, \dots, Z$ project each \tilde{b}_k onto the lognormal density to find $\tilde{\theta}_k$, and compute $\hat{\delta}_k$ from $\tilde{\theta}_k$.

Step 6. For each $k = 1, 2, \dots, Z$, calculate the bilinear interpolation weight for $\tilde{\delta}_k$ on G . For each $\tilde{\delta}_k$, sum the bilinear interpolation weight.

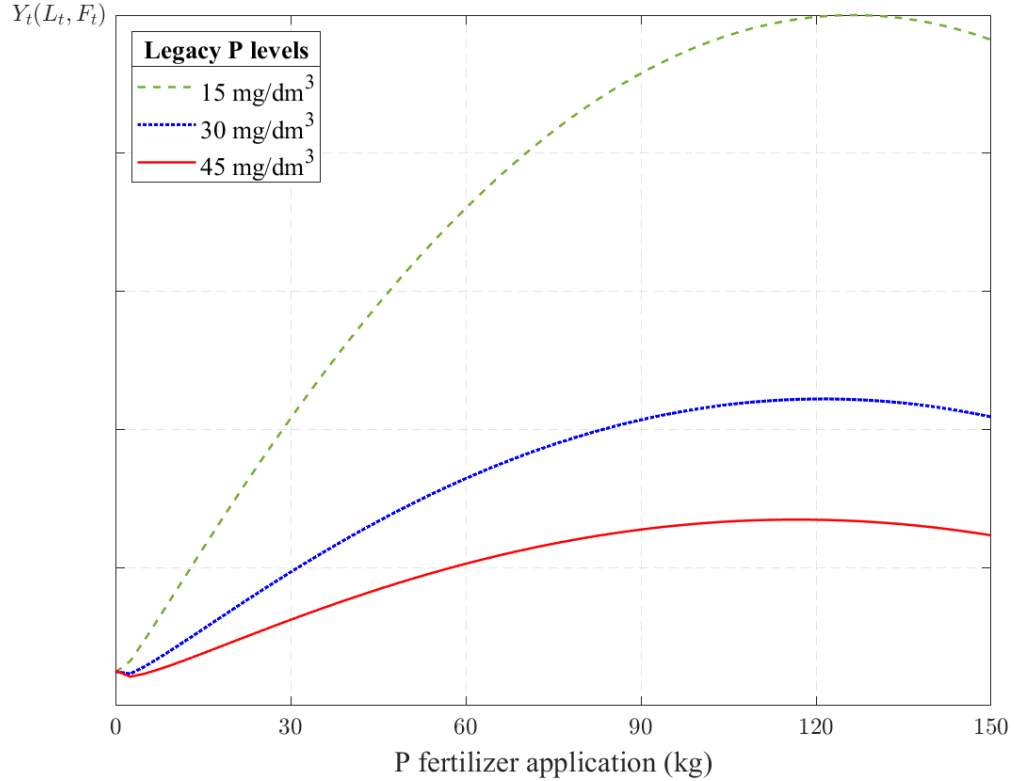
$$\tilde{p}(\delta_i, F, s)(\delta_j) = \frac{\text{sum of bilinear interpolation weights assigned to } \delta_j}{Z}$$

Source: Zhou et al. (2010), Kling et al. (2017)

Based on the output from Algorithm 2. and the estimated transition probabilities of corn and P fertilizer price, we proceed to calculate the comprehensive of transition probabilities $p(P^{F'}|P^F)p(P^{Y'}|P^Y)\tilde{p}(\delta_i, F, s)(\delta_j)$. The combination of these probabilities is achieved through the Kronecker delta product of probability matrices for corn and P fertilizer prices, as well as the transition probabilities $\mathbf{P}^Y \otimes \mathbf{P}^F \otimes \tilde{\mathbf{P}}$ (Sloggy et al. 2020), where \mathbf{P}^Y and \mathbf{P}^F are the probability matrix for corn and P fertilizer price, and $\tilde{\mathbf{P}}$ is the estimated probability matrix of $\forall i, j, \tilde{p}(\delta_i, F, s)(\delta_j)$.

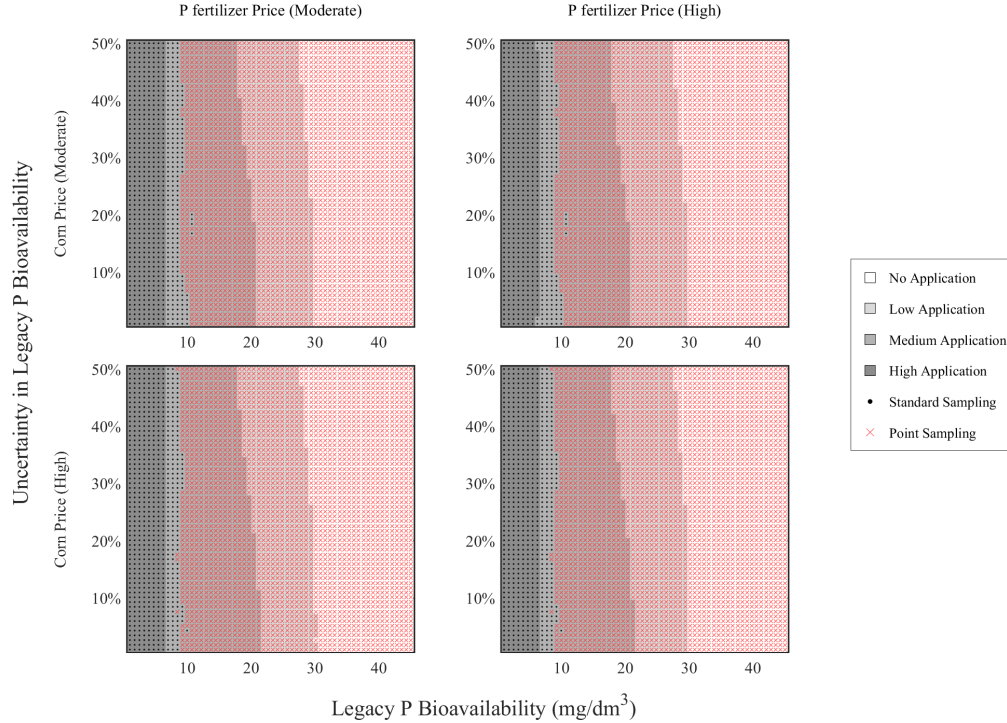
B Supplementary Figures

Figure B1: Response of legacy P on crop yield response to P fertilizer application



Notes: Figure A1 shows crop yields as a function of P fertilizer application across three levels of soil legacy P. Yields increase with more P fertilizer but at a decreasing rate, indicating diminishing returns, especially at high legacy P levels. The curves-blue for 15mg/dm³, red for 30mg/dm³, and green for 45mg/dm³-illustrate lower yield benefits from additional P fertilizer when legacy P is already high.

Figure B2: Response of legacy P on crop yield response to P fertilizer application



Notes: : In the original model, the standard deviation $\sigma_\rho(L)$ of the log percentage growth rate is inversely related to the legacy P level (equation 2), reflects an assumption in the model that more abundant legacy P stocks are assumed to be relatively more predictable in terms of their carry-over to the next period. Because we have no quantitative data with which to estimate the form of $\sigma_\rho(L)$, we investigate the effects of the alternative assumption that $\sigma_\rho(L) = \varsigma$ is fixed at uncertainty coefficient. This figure shows the model output derived under the alternative assumption. Given the uncertainty regardless in the dynamics scaling with legacy P levels, an optimal approach is to employ substantially more intensive soil sampling across state spaces.

Figure B3: Risk analysis: Epstein-Zin preference (moderate corn price \times high P fertilizer)

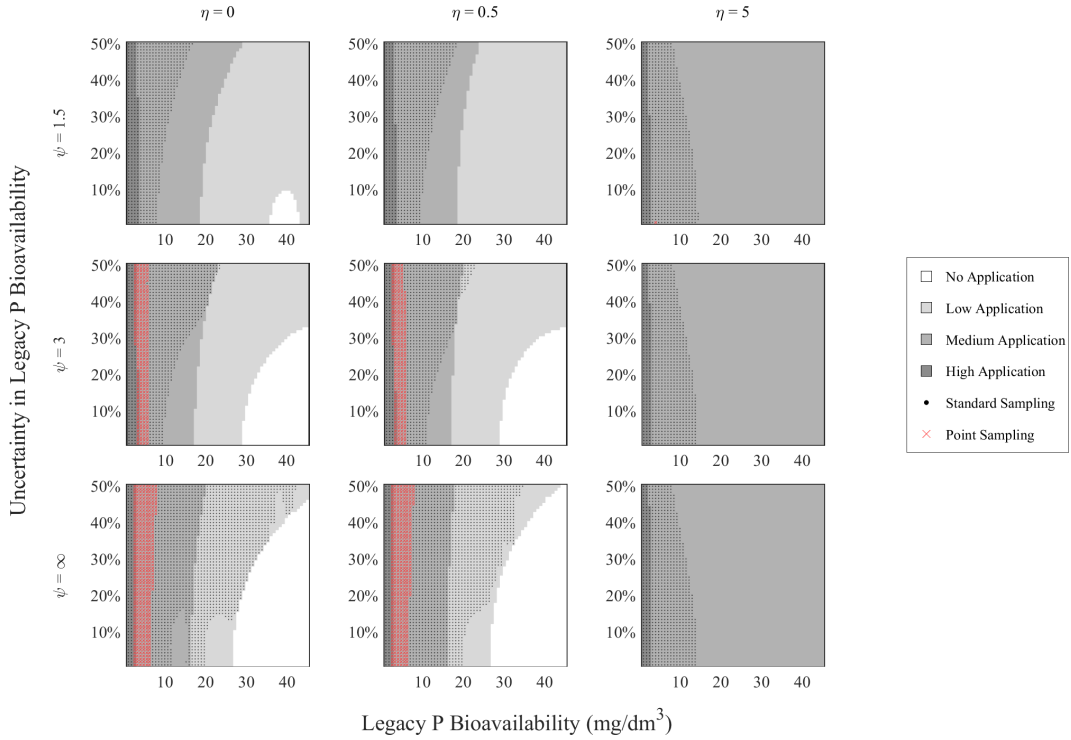


Figure B4: Risk analysis: Epstein-Zin preference (high corn price \times moderate P fertilizer)

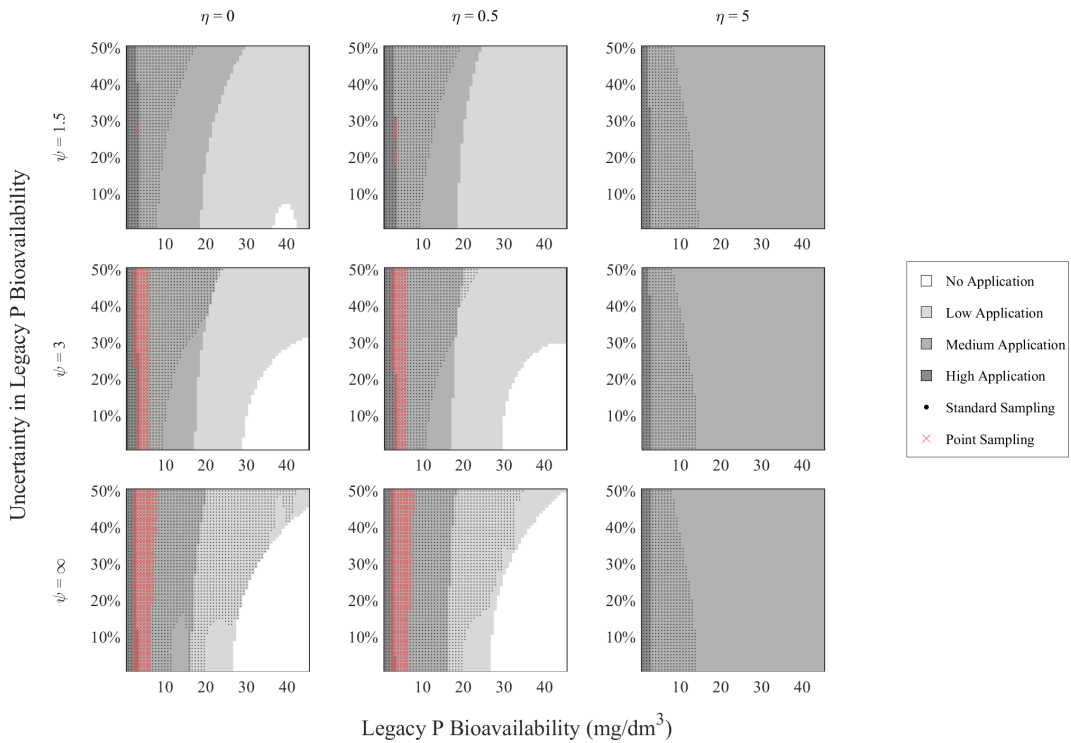


Figure B5: Risk analysis: Epstein-Zin preference (high corn price \times high P fertilizer)

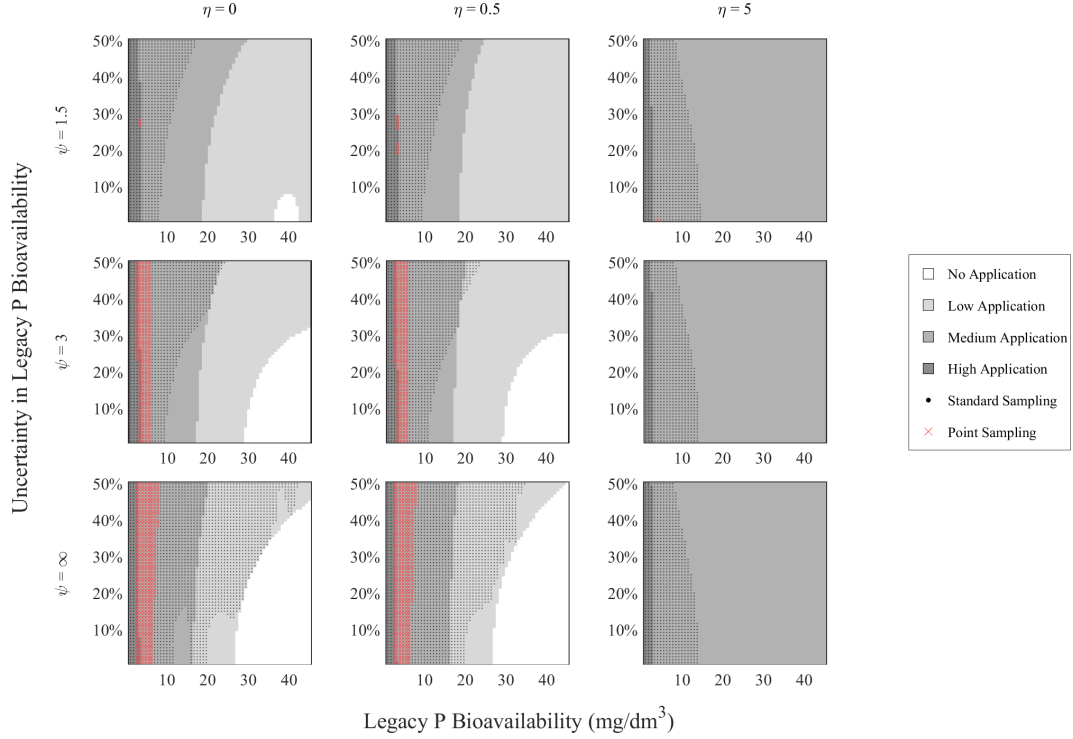


Figure B6: Dynamics of legacy P bioavailability (moderate corn price \times high P fertilizer price)

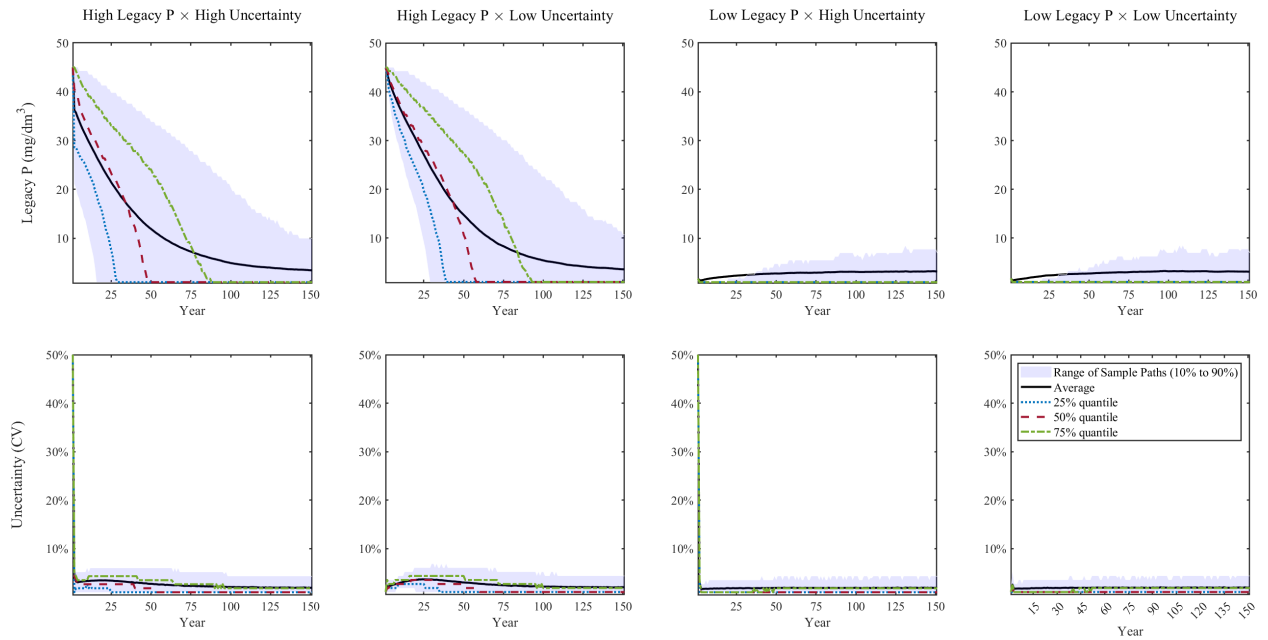


Figure B7: Dynamics of legacy P bioavailability (high corn price \times moderate P fertilizer price)

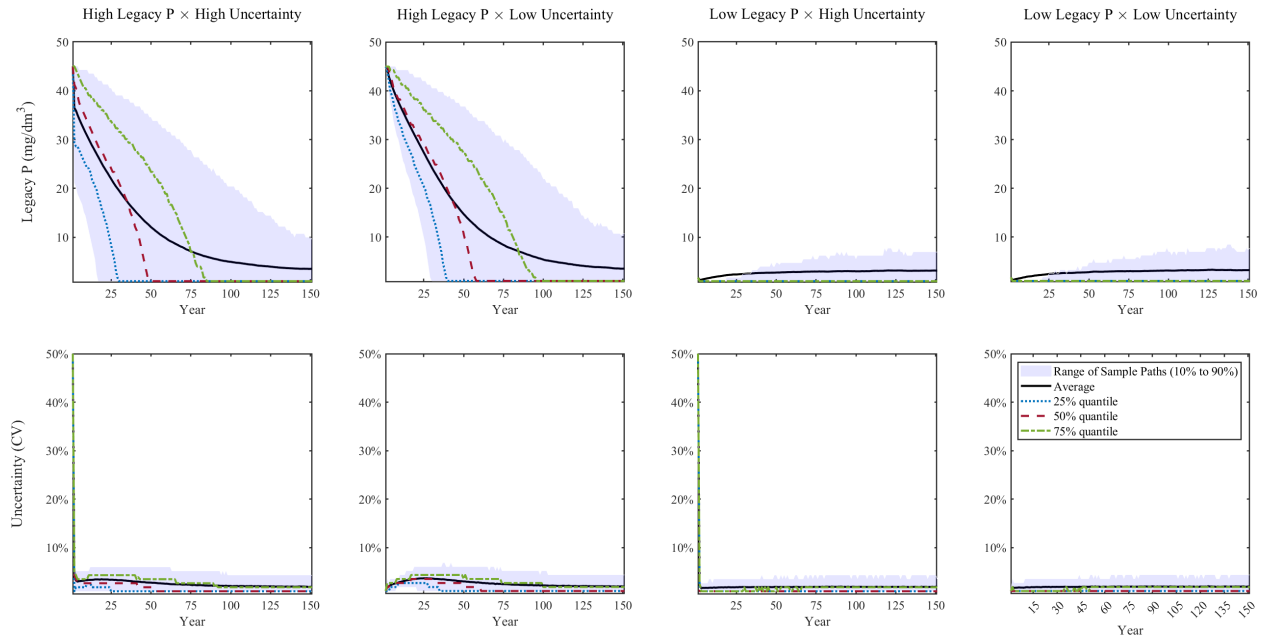


Figure B8: Dynamics of legacy P bioavailability (high corn price \times high P fertilizer price)

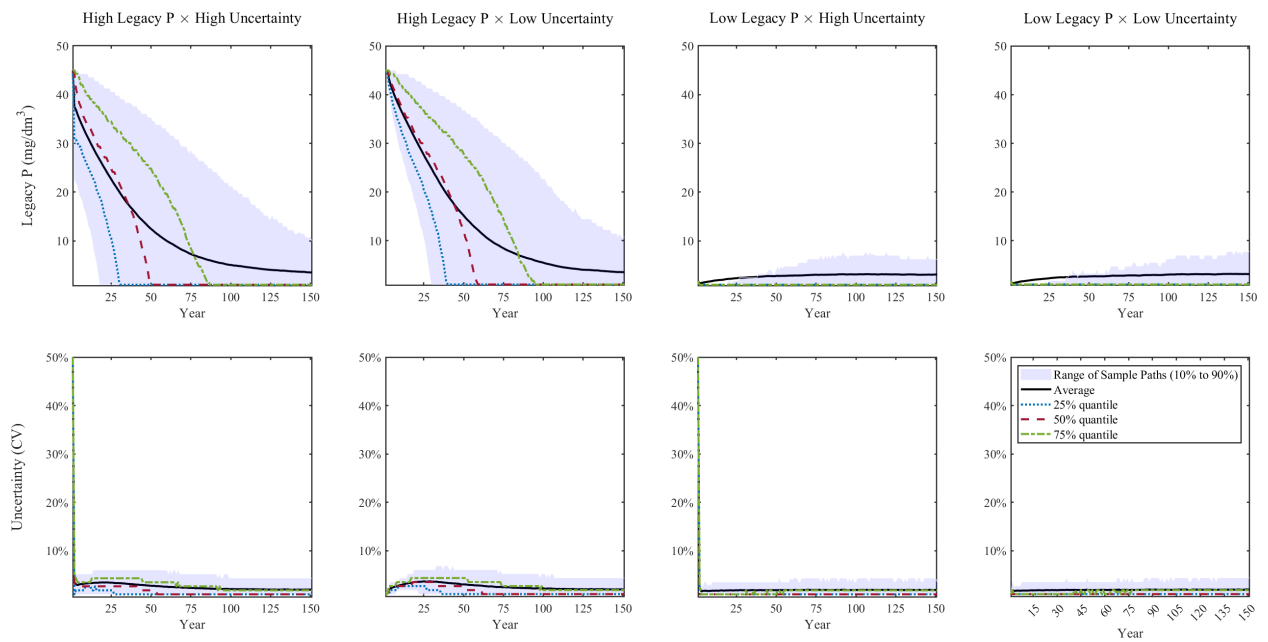


Figure B9: Risk neutral farmer responses to increased P fertilizer tax (moderate corn price and high P fertilizer price)

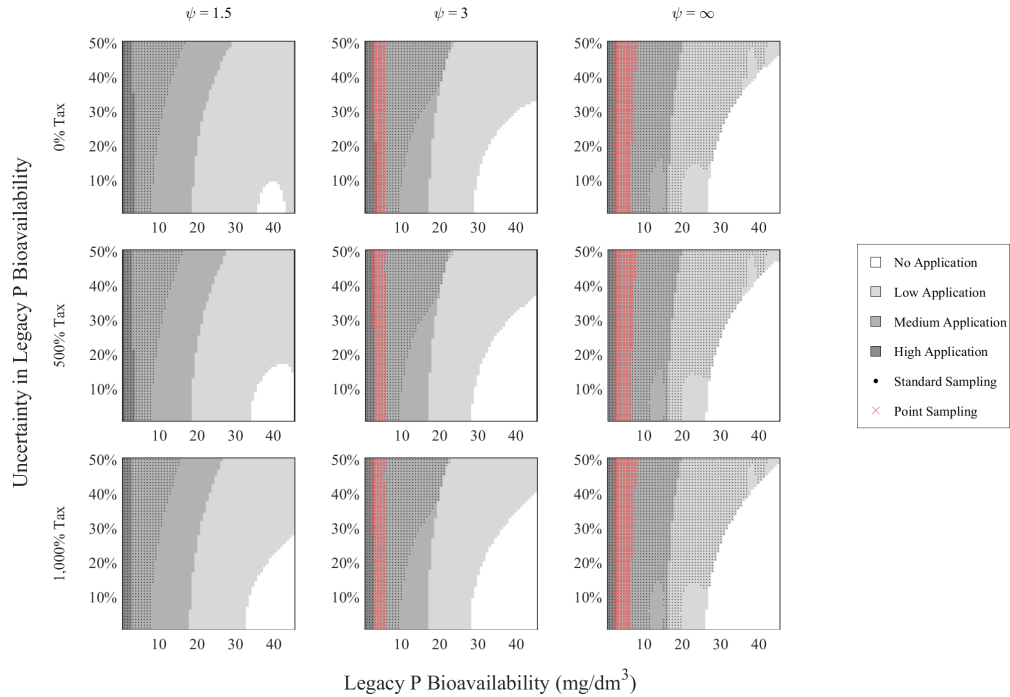


Figure B10: Risk neutral farmer responses to increased P fertilizer tax (high corn price and moderate P fertilizer price)

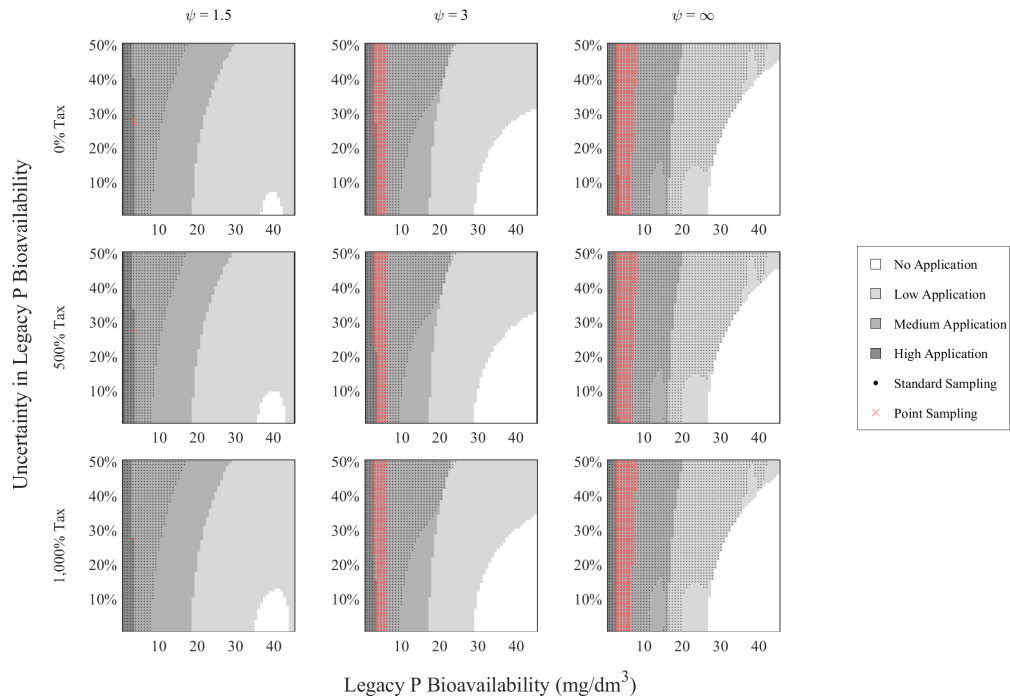


Figure B11: Risk neutral farmer responses to increased P fertilizer tax (high corn price and high P fertilizer price)

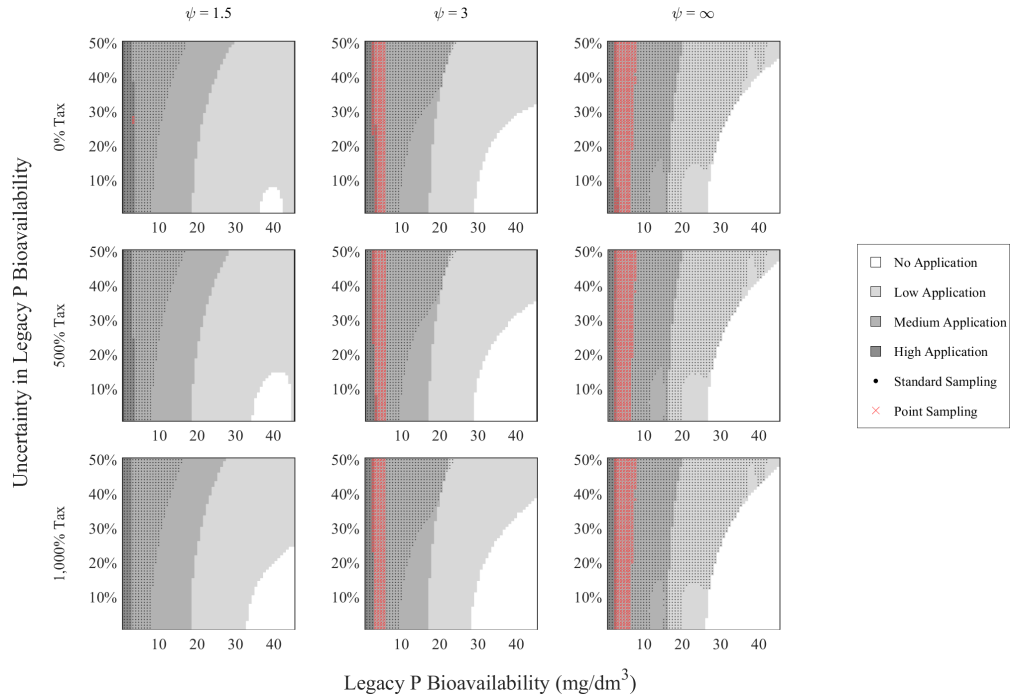


Figure B12: Risk-averse farmer responses to soil sampling subsidy (moderate corn price and high P fertilizer price)

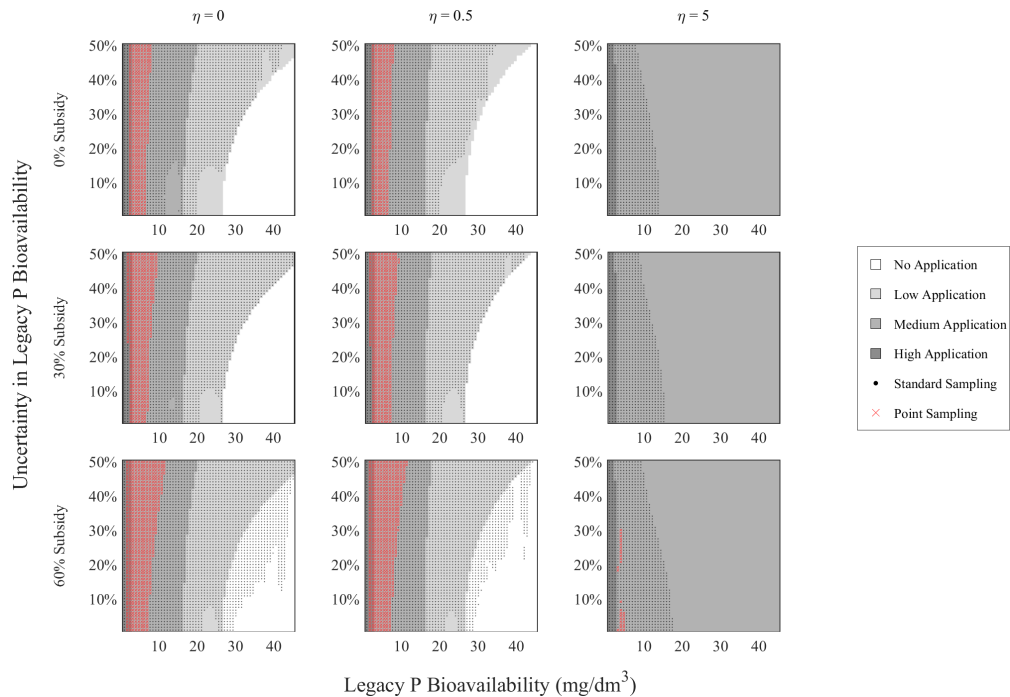


Figure B13: Risk-averse farmer responses to soil sampling subsidy (high corn price and moderate P fertilizer price)

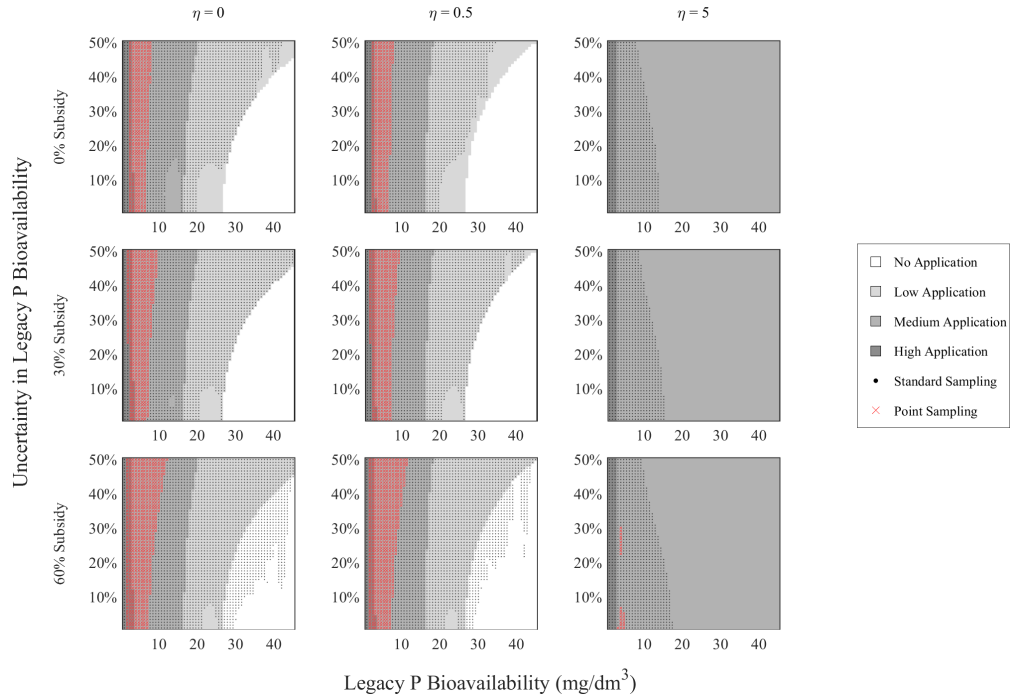


Figure B14: Risk-averse farmer responses to soil sampling subsidy (high corn price and high P fertilizer price)

